Palaeogeography, Palaeoclimatology, Palaeoecology 659 (2025) 112660

Contents lists available at ScienceDirect

Palaeogeography, Palaeoclimatology, Palaeoecology

journal homepage: www.elsevier.com/locate/palaeo

Planktic foraminiferal response to the Early Eocene Climatic Optimum (EECO) from southern mid-to-high latitudes

Giulia Filippi *, Valeria Luciani

Department of Physics and Earth Sciences, University of Ferrara, Via Saragat 1, Ferrara, Italy

ARTICLE INFO

Editor: L Angiolini

Keywords:
Planktic foraminifera
Abundance
Stable isotope
High latitudes
Poleward migration
EECO

ABSTRACT

The Early Eocene Climatic Optimum (EECO; ~53–49 Ma) records the warmest long-term global average temperature and CO_2 levels of the Cenozoic and is punctuated by multiple transient global warming events (hyperthermals), providing a significant opportunity to investigate the impact of extreme heat on planktic foraminifera, a key group of marine calcifiers highly sensitive to paleoenvironmental changes. Studies on Atlantic and Pacific Oceans documented a dramatic decline in abundance and diversity of the symbiont-bearing genus *Morozovella* close to the EECO onset (J event), and a corresponding permanent increase in the abundance of *Acarinina*. We extend the record to southern high-latitude locations on the Australia margin to provide a global perspective on planktic foraminiferal resilience to the EECO. We present planktic foraminiferal biostratigraphy, quantitative abundance and dissolution from Hole 762C (Exmouth Plateau, Indian Ocean) and Site U1510 (Tasman Sea, Pacific Ocean). Despite core breaks, these sites record multiple hyperthermals within the EECO. Our results suggest that cooler conditions at higher latitudes may have mitigated the decline of *Morozovella* observed at Atlantic and tropical Pacific sites. At Hole 762C and Site U1510, *Acarinina* dominates the assemblage, demonstrating the greatest ecological flexibility. The disappearance of the genus *Chiloguembelina* from the K/X hyperthermal through the EECO in the studied sites may represent a global event as it occurred at the same level in the Atlantic and tropical Pacific. This study from higher southern latitudes enhances our understanding of global planktic foraminiferal resilience to the EECO underlying similarities and differences constrained by the diverse geological settings.

1. Introduction

The fossil record reveals significant changes in response to climatic shifts during the early Eocene, with warming events leading to varied and often complex effects on species and ecosystems (e.g., Schmidt et al., 2004; Finkel et al., 2007; Agnini et al., 2009; McInerney and Wing, 2011; Speijer et al., 2012; Norris et al., 2013). In this respect, the Early Eocene Climatic Optimum (EECO; ~53–49 Ma), is a critical interval for understanding the biotic responses to extreme warmth, as it represents the prolonged peak of global mean temperatures during the Cenozoic (Slotnick et al., 2015; Lauretano et al., 2016; Luciani et al., 2016; Westerhold et al., 2018; Hollis et al., 2019). The sea surface temperatures were at their warmest long-term state due to high atmospheric CO_2 levels, reaching values between 1170 and 2490 ppm (Anagnostou et al., 2020; Miller et al., 2020; Hönisch et al., 2023; CenCO2PIP, 2023). Global mean surface temperature estimates for the EECO (27.0 °C) are ~10 to ~16 °C warmer than the Holocene (Inglis et al., 2020; Gaskell et al., 2022). The high atmospheric CO_2 levels resulted in increased concentrations of dissolved CO_2 in the ocean and in turn lower pH (e.g., Pearson and Palmer, 2000; Anagnostou et al., 2020; Rae et al., 2021). Several short-lived warming events (hyperthermals) are superimposed on the early Eocene warming (e.g., Zachos et al., 2005, 2010; Littler et al., 2014). These hyperthermals (Thomas, 1998) share several key characteristics, most notably negative carbon isotope ($\delta^{13}C$) excursions (CIEs) and evidence for dissolution of deep-sea carbonate related to Carbonate Compensation Depth (CCD) rise (e.g., Zachos et al., 2005; Leon-Rodriguez and Dickens, 2010). The Paleocene Eocene Thermal Maximum (PETM, ~ 56 Ma) is the most prominent example (e.g., Zachos et al., 2005, 2010; Kirtland-Turner et al., 2014) and it is followed by several hyperthermals, such as the Eocene Thermal Maximum 3 (ETM3; ~52.4 Ma) also known as the K- or X-event (Cramer et al., 2003; Rohl et al., 2005), and the J Event (53.26 Ma; Thomas et al., 2018; Westerhold et al., 2018), commonly considered to mark the EECO beginning (Slotnick et al., 2012, 2015; Lauretano et al., 2016; Luciani et al., 2016).

* Corresponding author.
E-mail address: giulia.filippi@unife.it (G. Filippi).

https://doi.org/10.1016/j.palaeo.2024.112660
Received 30 September 2024; Received in revised form 25 November 2024; Accepted 5 December 2024
Available online 8 December 2024

Nomenclature: List of Species Cited in Text and Figures

Acarinina Subbotina, 1953.
Catapsydrax Bolli, Loeblich and Tappan, 1957.
Chiloguembelina Loeblich and Tappan, 1956.
Globanomalina Haque, 1956.
Globanomalina planoconica (Subbotina, 1953).
Guembelitrioides nuttalli (Hamilton, 1953)
Igorina Davidzon, 1976.
Morozovella aequa (Cushman and Renz, 1942).
Morozovella aragonensis (Nuttall, 1930).
Morozovella caucasica (Glaessner, 1937).
Morozovella crater (Hornibrook, 1958).
Morozovella formosa (Bolli, 1957).
Morozovella gracilis (Bolli, 1957).
Morozovella lensiformis (Subbotina, 1953).
Morozovella marginodentata (Subbotina, 1953).
Morozovella subbotinae (Morozova, 1939).
Parasubbotina Olsson et al., 1992.
Parasubbotina inaequispira (Subbotina, 1953).
Parasubbotina varianta (Subbotina, 1953).
Planorotalites Morozova, 1957.
Pseudohastigerina Banner and Blow, 1959.
Subbotina Brotzen and Pozaryska, 1961.
Subbotina senni (Beckmann, 1953).

This EECO interval is important for understanding the resilience of long-term extreme warmth on marine organisms, particularly the planktic foraminifera, which play a role in the marine carbon cycle through carbonate production and burial (Ridgwell and Zeebe, 2005). The impact of warming on planktic foraminifera may include species migration towards higher latitudes and deeper waters, changes in growth and reproduction, and, in some cases, local extinctions (Jonkers et al., 2019; Woodhouse et al., 2021; Cooley et al., 2022; Chaabane et al., 2023). As a result, planktic foraminifera are widely used to reconstruct the impact of past environmental changes on marine ecosystems (Kucera, 2007; Chaabane et al., 2023).

The genera *Morozovella* and *Acarinina* were symbiont-bearing mixed-layer planktic foraminifera which dominated early Paleogene tropical and subtropical surface oceans (Boersma et al., 1987; Premoli Silva and Boersma, 1988; Pearson et al., 2006). During the EECO, these genera exhibit a permanent switch in their abundance and diversity across the Atlantic Ocean, Tethys realm, and the tropical Pacific Ocean, with *Morozovella* experiencing a sharp decline while *Acarinina* becomes dominant, with the former reducing diversity and the latter increasing the species number (Pearson et al., 2006; Aze et al., 2011; Fraass et al., 2015; Luciani et al., 2016, 2017a, 2017b; D'Onofrio et al., 2020; Filippi et al., 2024). The deeper-dweller genus, *Chiloguembelina,* which radiates in the middle Eocene and ranges up to the Oligocene, (e.g., King and Wade, 2017; Pearson et al., 2006; Fucek et al., 2018) virtually disappears from several latitudes of the Atlantic and tropical Pacific Ocean within the EECO (Luciani et al., 2020a, 2020b; Filippi et al., 2024).

To provide a broader understanding of how global climatic shifts have influenced the resilience of marine ecosystems across different ocean basins, we present here planktic foraminiferal data from southern latitudes that were so far lacking, though being essential to document the global planktic foraminiferal response to the EECO.

Specifically, we selected the Ocean Drilling Program (ODP) Hole 762C (Exmouth Plateau, Indian Ocean) and International Ocean Discovery Program (IODP) Site U1510 (Lord Howe Rise, Tasman Sea, Pacific Ocean; Fig. 1).

The study of Hole 762C benefits from published records including stable isotope analyses, though at low resolution (Thomas et al., 1992; Hancock et al., 2002; Fig. 1), nannofossil zonation and major changes in nannofossil assemblages (Shamrock et al., 2012) together with updated magnetostratigraphy and data on Eastern Indian Ocean dynamics (Xu et al., 2021). During the early Eocene, Hole 762C was influenced by the proto-Indian Ocean gyre, resulting in highly oligotrophic conditions

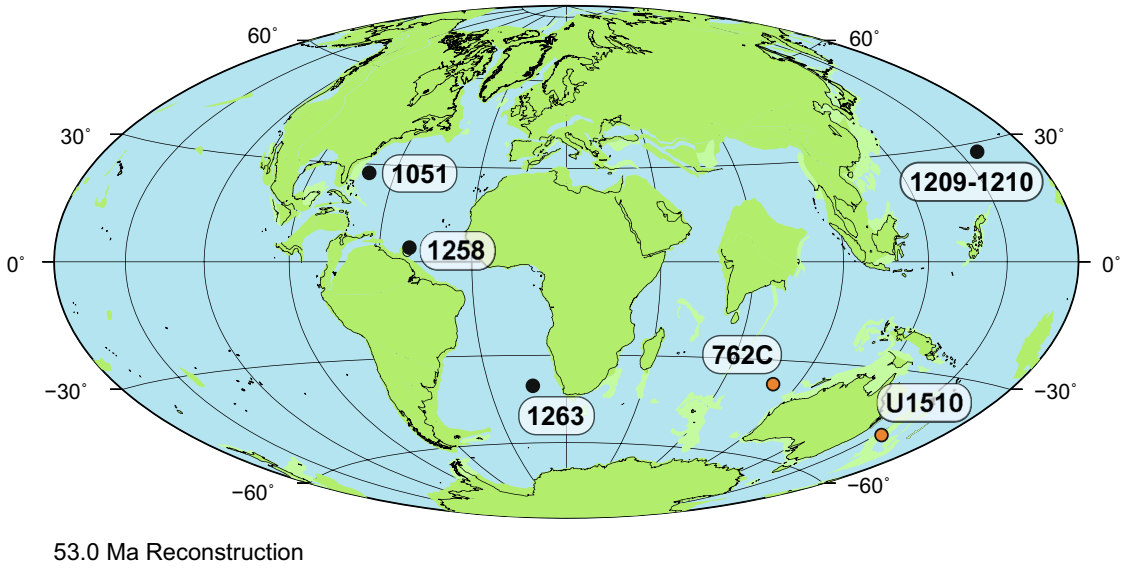

Fig. 1. Approximate location of the studied sites ODP Hole 762C, Exmouth Plateau (Indian Ocean), and IODP Site U1510, Lord Howe Rise (Tasman Sea, southwestern Pacific Ocean), approximately during the early Eocene (orange dots). Also shown are the locations of ODP Atlantic sites 1051, 1258 and 1263, and tropical Pacific Sites 1209–1210 (black dots), where planktic foraminiferal records show a major change in genera across the EECO and $\delta^{13}C$ records are detailed (D'Onofrio et al., 2020; Luciani et al., 2017a, 2017b; Filippi et al., 2024). The base map is from https://www.odsn.de/odsn/services/paleomap/adv_map.html with paleolatitudes modified for sites 1051, 1263, 1258, 1209–1210, U1510 and Hole 762C are according to www.paleolatitude.org model version 1.2 (Van Hinsbergen et al., 2015). Note that locations might be adjusted to a different reference frame to account for changes in plate motion relative to the spin axis (Hollis et al., 2012).

with full nutrient consumption (Müller et al., 2019). This interpretation is supported by nannofossil data from Shamrock et al. (2012). The high latitude location of Hole 762C may have induced some species to reach the limits of their biogeographic ranges (Wonders, 1992; Hancock et al., 2002).

The southwest Pacific Site U1510 was in proximity to a deep water formation area in the Southern Ocean sector during the early Eocene (Huck et al., 2017; Fig. 1). The early Eocene conditions in the Tasman Sea were characterized by gyral circulation without significant throughflow through the Tasmanian Gateway (Bijl et al., 2013; Huber et al., 2004). Increased southward expansion of a warm proto-East Australian Current has been suggested to explain peak warmth in the early Eocene (Hines et al., 2017; Hollis et al., 2012). TEX86-based sea surface temperatures (SSTs) from marginal marine sediments of the East Tasman Plateau and mid-Waipara (New Zealand) indicate near-tropical conditions (between 24 °C and 31 °C) during the EECO (Bijl et al., 2013). Peak EECO warmth at the mid-Waipara River section coincides with an increase in warm-water calcareous nannofossil and dinocyst taxa, and a high abundance of planktic foraminifera (Crouch et al., 2020; Hollis et al., 2009, 2012).

Site U1510 was selected for its paleoceanographic setting in southern latitude of Pacific Ocean, the availability of stable isotope records, which allow the identification of the main CIEs, and benthic foraminifera and calcareous nannofossils data (Alegret et al., 2021a, 2021b).

We present new data on planktic foraminiferal biostratigraphy, quantitative abundance of taxa and fragmentation index, as dissolution proxy, from the two selected sites besides new detailed bulk stable isotopes from Hole 762C. By comparing these locations with the documented changes in the Atlantic and tropical Pacific Oceans, we aim to determine whether similar patterns of planktic foraminifera response to the EECO environmental changes can be detected at southern latitudes.

Furthermore, we provide new information on the paleoecology of *Globanomalina* based on stable isotope data generated for the EECO interval at Site U1510.

2. Material and methods

2.1. Site locations

ODP Hole 762C was drilled on the central Exmouth Plateau (19°53.24′S, 112°15.24′E) at a water depth of 1360 m (Shipboard Scientific Party, 1990) (Fig. 1). The sediments from this Hole consist of nannofossil chalks and ooze (Shipboard Scientific Party, 1990; Siesser and Bralower, 1992). Our analysis included ~~81~~ 85 samples taken from 413.023 m below the seafloor (mbsf) to 313.05 mbsf, spanning the early Eocene interval. The sampling resolution was approximately 50 cm across hyperthermal events and 100 cm between them (Table S1). Even though the lack a detailed age model for Hole 762C during the EECO, our 50 cm space sampling corresponds to roughly 50 kyrs, based on the age of global carbon isotope excursions (CIEs) according to Westerhold et al. (2018).

This site records several CIEs below and within EECO, although some sections are affected by core breaks (Shipboard Scientific Party, 1990; Thomas et al., 1992; Hancock et al., 2002). The southern mid-latitude paleo-location on the northwest margin of Australia, and the good preservation of planktic foraminifera (Hancock et al., 2002) make this site particularly valuable for providing a global perspective on planktic foraminiferal resilience during the EECO. The planktic foraminiferal zonation adopted by Hancock et al. (2002) is from the zonal scheme by Berggren et al. (1995) (P for Paleogene zones) and was to be updated with the most recent zonal scheme by Wade et al. (2011) (E Eocene zones). Calcareous nannofossil biostratigraphy was provided by Siesser and Bralower (1992) according to Martini (1971) biozonation. Recalibrated magnetostratigraphy (Xu et al., 2021) and low-resolution bulk and *Subbotina* carbon isotopes, come from Thomas et al. (1992) and Hancock et al. (2002) respectively.

Additionally, we analyzed pelagic cores of International Ocean Drilling Program (IODP) Site U1510, located on southern Lord Howe Rise (36°19.74′S, 164°33.52′E) drilled at 1238 m water depth, ~850 km west of northern New Zealand (Sutherland et al., 2018, Sutherland et al., 2019a, Sutherland et al., 2019b; Fig. 1). Alegret et al. (2021) provide benthic and bulk stable isotope curves. This site records the K event (~52.4 Ma), S (~50.4 Ma), T (~50.37 Ma), and U (~49.95 Ma) CIEs (Alegret et al., 2021a, 2021b). A core gap is present between 473.790 and 468.800 CFS. Coring disturbance in Cores U1510- 51× and -52×, combined with the very low magnetic remanence, hampered a reliable magnetic polarity age control (Sutherland et al., 2019a). We analyzed 27 samples, the same adopted by Alegret et al. (2021a, 2021b), generally consisting of nannofossil chalk, in Cores U1510-51× and 52× from 477.82 to 464.24 mbsf converted in Corrected sea Floor (CSF) due to core gaps (Alegret et al., 2021b). The sampling spacing is of 20–60 cm (Table S2).

2.2. Stable isotope analysis

Carbon and oxygen stable isotopes from Hole 762C were performed on bulk sediments at Ferrara University, Italy, through the Elemental Mass Spectrometer© isoprime precisION with a centrION system, isoFLOW Equilibration System, and ionOS® IRMS Software the Stable Isotope. Samples were first freeze-dried and then pulverized manually with a mortar. Samples of ~200–250 μg were flushed with helium and then treated with 10 mL of 100 % phosphoric acid (EMSURE ® ≥ 99 %) at 70 °C for ca. 3 h. Isotopic values are reported in standard delta notation relative to the Vienna Pee Dee Belemnite (VPDB). During the analyses an internal standard (white Carrara marble Maq 1: $\delta^{13}C = +2.58$ ‰; $\delta^{18}O = -1.15$ ‰ VPDB) was used to normalize raw $\delta^{13}C$ and $\delta^{18}O$ values and a check standard (marble Gr1: $\delta^{13}C = +0.69$ ‰; $\delta^{18}O = -10.63$ ‰ VPDB) was run for quality assurance, and repeated with precisions better than ±0.05 ‰ for $\delta^{13}C$, and better than ±0.08 ‰ for $\delta^{18}O$. Raw data are shown in Table S1.

Bulk stable Isotopes analyses at Site U1510 were performed by Alegret et al. (2021a, 2021b) on a total of 54 samples using a Thermo Fisher Scientific MAT 253 with a Kiel IV carbonate device at the University of California, Santa Cruz. Long-term reproducibility in standards (e.g., Carrara Marble) indicates precision for $\delta^{13}C$ and $\delta^{18}O$ (1σ) of ±0.05 ‰ and ± 0.08 ‰, respectively.

Benthic Stable Isotope data are also from Alegret et al. (2021a, 2021b), using a ThermoFisher Scientific 253plus gas isotope ratio mass spectrometer with Kiel IV automated carbonate preparation device at MARUM. Samples were reacted with orthophosphoric acid at 75 °C. Analytical precision based on replicate analyses of in-house standard (Solnhofener Limestone) averages 0.03 ‰ and 0.04 ‰–0.06 ‰ (1σ) for $\delta^{13}C$ and $\delta^{18}O$, respectively. Data are reported relative to the Vienna Pee Dee Belemnite international standard, determined via adjustment to calibrated in-house standards and NBS-19 (Alegret et al., 2021a, 2021b).

In addition, we performed carbon and oxygen stable isotopic analysis on *Morozovella*, *Acarinina*, *Subbotina* and *Globanomalina* genera from Site U1510 on the size fraction ≥150 μm (Table S6). Samples were selected with respect to their collocation to the X event: one sample below (477.83 CSF), two samples across the CIE (476.96 and 476.31 CSF), one sample at the top of the event, and two samples in the post X (475.93 and 474.99 CSF). A quantity of 120–180 μg was picked for each taxon. Taxa were identified according to Pearson et al. (2006). $\delta^{13}C$ and $\delta^{18}O$ values were obtained at the Stable Isotope Laboratory of the Department of Geosciences at the University of Padova using a Thermo Scientific Delta V Advantage Isotope Ratio Mass Spectrometer coupled with a Gas Bench II automated preparation device on bulk samples. Samples were first freeze-dried and then pulverized manually with a mortar. Samples ≥150 μg were flushed with helium and then treated with 10 mL of 100 % phosphoric acid (EMSURE ® ≥ 99 %) at 70 °C for about 3 h. Isotopic values are reported in standard delta notation relative to the Vienna Pee Dee Belemnite (VPDB). During the analyses an internal standard (white

Carrara marble Maq 1: $\delta^{13}C = +2.58$ ‰; $\delta^{18}O = -1.15$ ‰ VPDB) was used to normalize raw $\delta^{13}C$ and $\delta^{18}O$ values and a check standard (marble Gr1: $\delta^{13}C = +0.69$ ‰; $\delta^{18}O = -10.63$ ‰ VPDB) was run for quality assurance and repeated with precisions better than 0.03 ‰ for $\delta^{13}C$, and better than 0.05 ‰ for $\delta^{18}O$.

2.3. Carbonate dissolution proxy: Fragmentation Index

Planktic foraminifera test fragmentation is a result of deep-sea carbonate dissolution, commonly associated with early Eocene negative CIEs (e.g., Berger, 1970; Hancock and Dickens, 2005; Nguyen and Speijer, 2014). Differences in the susceptibility to dissolve of various genera or species could potentially bias the assemblage of records (e.g., Nguyen et al., 2009, 2011; Petrizzo et al., 2008). We adopt the fragmentation index (F index) as a dissolution proxy (Berger, 1970) which is the ratio between fragments or partially dissolved planktic foraminiferal tests versus entire tests on ~300 individuals ≥63 μm and expressed as a percentage (Tables S1, S2) from 39 samples at Hole 762C and 24

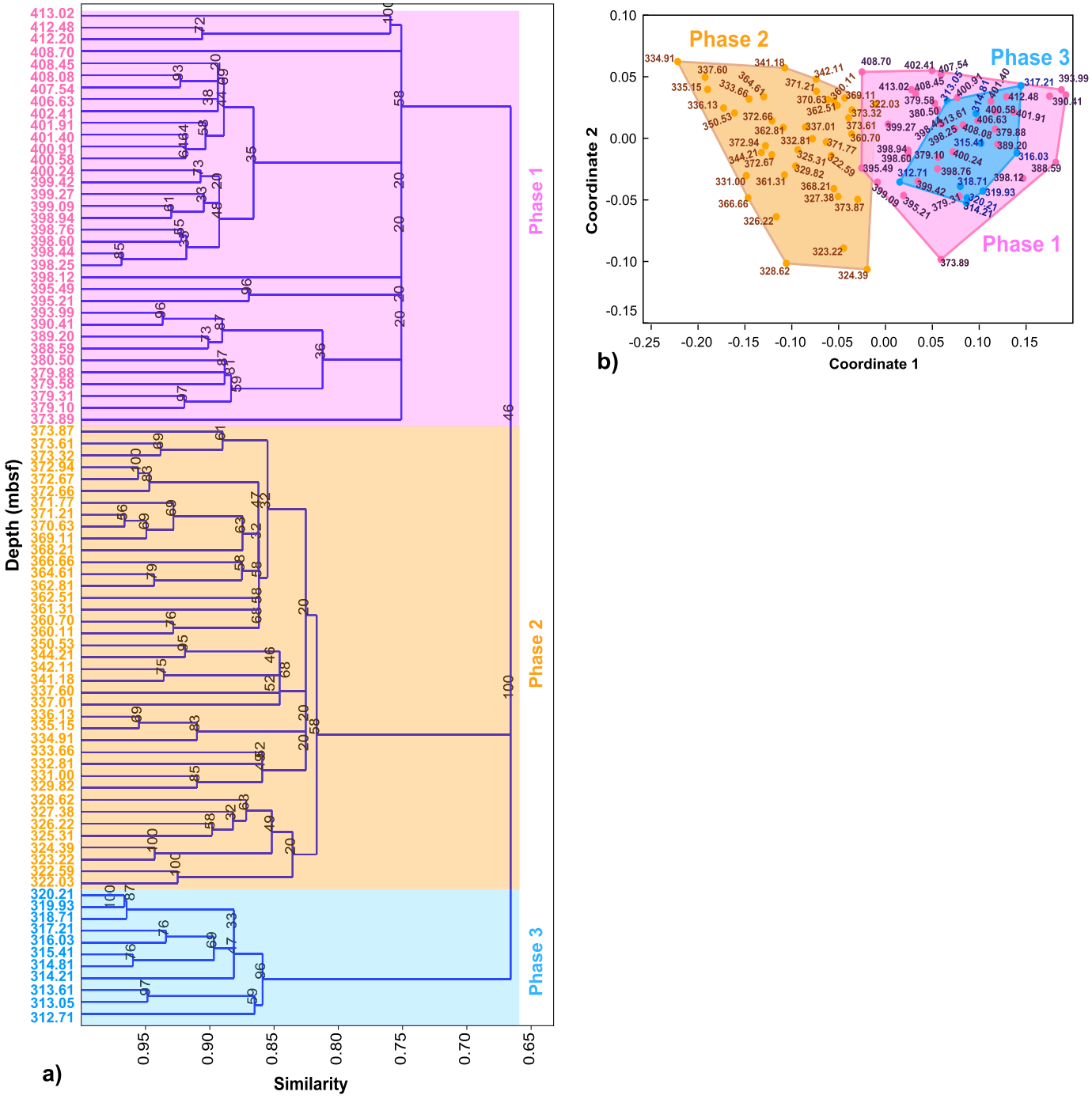

Fig. 2. a) Dendrogram of the stratigraphically-constrained multivariate classical clustering analysis performed on planktic foraminiferal most abundant genera (*Morozovella, Acarinina* and *Subbotina)* relative abundances (%) across the studied interval, using a Paired Group (UPGMA) algorithm and the Bray-Curtis similarity index, with the main clusters named and highlighted with different colours coinciding with Phases 1, 2, 3 shown in Fig. 3. Node values are for 1000 bootstraps. The numbers at the top of the dendrogram correspond to the sample depths, ordered in increasing order from left to right **b)** Clusters recovered by non-metric multidimensional scaling ordination analysis, using the Bray-Curtis similarity index, with hulls and labels representing groups recovered in Fig. 2a. Dots represents individual samples, with each dot corresponding to the phase it belongs to as identified in the dendrogram in Fig. 2a.

samples at Site U1510.

2.4. Planktic foraminiferal analysis

Bulk samples from Hole 762C were oven-dried at 45 °C, weighed, and then immersed in deionized water. Disaggregation occurred from a few hours to three days, depending on the compactness of the sediments. When disaggregated, samples were washed over stacked ≥63 and ≥ 38 μm sieves. After each wash, sieves were immersed in a methylene blue bath to assess contamination (e.g., Green, 2001). The separated fractions of each washed residue were dried at 45 °C.

Planktic foraminifera were studied from washed residues (≥63 μm fraction) using a Zeiss stereomicroscope STEMI 305 and the presence/absence of zonal markers was established (Tables S3, S4). The taxonomic criteria adopted to identify planktic foraminiferal genera and species follow Olsson et al. (1999) and Pearson et al. (2006). The early Eocene planktic foraminiferal biohorizons (Wade et al., 2011) can be identified at Hole 762C and U1510. However, cases of diachronism were recorded as documented in Luciani and Giusberti (2014), D'Onofrio et al. (2020), Luciani et al. (2017a, 2017b) and Filippi et al. (2024) (Text S1, S2, Tables S3, S4).

Relative abundances of planktic foraminiferal genera were determined on more than 300 specimens of the ≥63 μm size fraction from random splits generated by a microsplitter, in 81 samples at Hole 762C and 27 samples at Site U1510. Additional analysis of the fraction comprised from 38 μm and 63 μm was performed to check the occurrence of the small-sized *Chiloguembelina*. Foraminiferal relative abundance quantitative data are provided in Tables S1 and S2. In the genus *Subbotina* we do not include the species *Subbotina senni* as *S. senni* was a mixed-layer species that migrated to middle mixed-layer or deeper depths during gametogenesis, meaning it presents a different ecology with respect to the subbotinids groups (Pearson et al., 1993, 2006). In the subbotinids group, we include rare *Parasubbotina* specimens (*P. inaequispira, P. varianta*) as these species are known as having a thermocline habitat similar to *Subbotina* (e.g., Pearson et al., 2006, and references therein).

To identify clusters of similar ecological signatures and understand how similarity might change through time, we performed hierarchical clustering, paired group (UPGMA) algorithm, with Bray–Curtis similarity index on planktic foraminifera genera abundances across the studied interval at Site Hole 762C (Fig. 2) and U1510 (Fig. 5). We combined a non-metric multidimensional scaling (NMDS) ordination analysis using the Bray-Curtis similarity index to identify cluster robustness and recover similarities between faunal groups independently from the stratigraphic position, using the Software PAST 4.17 (Hammer et al., 2001) (Figs. 2b, 5b).The clustering was applied to the same 85 samples from Hole 762C and 27 samples from Site U1510 that were analyzed for planktic foraminifera abundances (see paragraph 2.1 for sampling details). The analysis specifically focused on variations in the abundances of the dominant genera *Acarinina*, *Morozovella*, and *Subbotina*, which are the major contributors to the ecological patterns observed across the interval.

To discriminate between the main phases, we used the major branching points in the lower part of the dendrogram, with similarity values <0.75 at both sites, which represent the largest dissimilarities between groups with Similarity values. These branches allowed us to identify the main clusters. The primary groups highlighted in the dendrogram reflect significant changes in the relative abundances of the dominant genera (*Morozovella*, *Acarinina*, and *Subbotina*) and are corroborated by the NMDS ordination results, which confirm the robustness of the clusters independently of their stratigraphic position. At Site U1510, the distinction between "phases" and "subphases" is based on the level of clustering within the dendrogram. Phases correspond to major clusters formed at higher dissimilarity thresholds, while subphases are subdivisions within these clusters, reflecting finer ecological patterns at lower dissimilarity thresholds, with Similarity values <0.80. The stratigraphic boundaries of each phase extend up to the last sample included in the corresponding cluster (e.g., if Phase 1 spans from 413.02 mbsf to 373.89 mbsf, this phase ends at 373.89 mbsf, while the next sample marks the transition to Phase 2). It is important to note that the resolution of the sampling used for the cluster analysis is lower than that of other datasets analyzed in this study, such as the stable isotope curves. While this introduces a limitation in the resolution at which the ecological phases are defined, it reflects the resolution of the available data for planktic foraminifera abundances. Despite this, the clustering approach provides a framework for identifying major ecological shifts and grouping samples based on their faunal composition. The ecological phases identified are further quantified in Tables 2 and 3, which provide the mean values of genera abundances for each phase at Site Hole 762C and Site U1510, respectively. By presenting these mean values, Tables 2 and 3 allow for a comparative analysis of the ecological shifts of a genus abundance between phases, highlighting key differences in the planktic foraminiferal assemblages.

To verify the anti-phase fluctuations of *Acarinina* with *Morozovella* and *Subbotina* during the EECO we performed a co-occurrence matrix across the entire interval (Fig. S1), and a similarity heatmap with the abundance of these three genera during or close to the main CIEs (Fig. S2), using R Software, version 4.2.2. Supplementary Text S3.

3. Results

3.1. Stable isotopes at Hole 762C and U1510

The $\delta^{13}C$ values across Hole 762C ranges between ~ − 0.15 ‰ and ~ 2.92 ‰, with an average of 1.32 ‰ (Figs. 2, 4, Table S1). The $\delta^{18}O$ values at Hole 762C range between −1.69 ‰ to 0.85 ‰, with a mean value of −0.65 ‰ (Figs. 2, 4, Table S1). In Table S5 we identify the main EECO hyperthermals named following Westerhold et al. (2017) associated with the recorded CIEs. Events I2, J, and Q might not be present due to core gaps.

The $\delta^{13}C$ values across site U1510 are from Alegret et al. (2021a, 2021b) (Table S2). Fluctuations in the stable isotopes curve are correlated to the main CIEs identified by Alegret et al. (2021a, 2021b).

3.2. Fragmentation Index at Site 762C and U1510

The fragmentation at Site Hole 762C shows a mean value of ~21 % with a minimum of ~10 % at 379.31 mbsf and a maximum of ~39 % at 335.15 mbsf for the whole interval investigated at Hole 762C (Fig. 2, Table S1). High, above-average values are associated with some of the main CIEs (Table 1), or close to them.

The fragmentation at Site U1510 records average values of ~37 %, with a minimum value of ~7 % at 466.630 CSF-A and a peak value of 66 % at 477.33 CSF-A (K/X CIE; Fig. 5, Table S2). High, above-average

Table 1
Fragmentation Index (%) at Site Hole 762C and U1510 above average values (>21 % and > 37 % respectively). CIEs are identified in this work and labelled following Westerhold et al. (2017). At Site U1510 CIEs are according to Alegret et al. (2021a, 2021b).

SITE HOLE 762C			SITE U1510		
Depth (mbsf)	CIEs	Fragmentation (%)	CSF-A top depth (m)	CIEs	Fragmentation (%)
324.39		34	465.380	**U**	51
335.15		39	467.790		42
342.11	**P**	29	468.420	**S**	53
370.63		28	473.900		61
371.77		26	475.240		58
379.10	**J?**	18	476.530	**K/X**	58
395.21	**H2**	27	477.330	**K/X**	66
406.63		27	477.820		47
413.02		22			

values are generally associated with some of the main CIEs (Table 1).

3.3. Variations in abundance and cluster analysis of planktic foraminiferal taxa at Hole 762C

The analysis of planktic foraminiferal relative abundance across the EECO interval at Hole 762C (Figs. 2, 4; Tables 2, S1) shows significant shifts in abundance, specifically observed in the genera *Acarinina*, *Subbotina*, and *Chiloguembelina*, while *Morozovella* exhibits more stable trends for most of the studied interval. Superimposed on these long-term trends are more abrupt, short-lived fluctuations in taxa abundance, often in concomitance with the main CIEs.

Cluster analysis, based on the relative abundance of the dominant planktic foraminifera (*Morozovella*, *Acarinina*, and *Subbotina*), reveals three distinct phases that we highlight with different colours in Figs. 2, 3 and Table 1: pre-EECO and J event **Phase 1** (pink), EECO **Phase 2** (orange), and post-EECO **Phase 3** (light blue).

Phase 1 (413.02–373.89 mbsf) shows a stable trend in *Morozovella* abundance, with an average of ~12 %. The genus *Acarinina* fluctuates more frequently and records higher abundance values, while *Subbotina* dominates this phase.

In **Phase 2** (373.87–322.03 mbsf) *Morozovella* maintains a stable trend until reaching its highest value of 36 % at 324.39 mbsf. *Acarinina* dominates this phase, more than doubling its abundance compared to Phase 1 and reaching its peak values. In contrast, *Subbotina* experiences a decline, with a relatively stable trend followed by a slight increase towards the end of the phase (Tables 2, S1; Figs. 2, 3).

Phase 3 (320.21–312.71 mbsf) is characterized by a decreasing trend in *Morozovella* and *Acarinina* while *Subbotina* restores the high abundance recorded in Phase 1 (Tables 2, S1; Figs. 2, 3). Phase 3 is located inside Phase 1 in the NMDS (Fig. 3b) suggesting similarity between these two clusters whereas the minimal overlap between Phase 2 and Phase 1 indicates very low correspondence.

On shorter timescales, *Acarinina* abundance often fluctuates in antiphase with *Morozovella* and *Subbotina*, particularly during the CIEs. The co-occurrence matrix and heatmap in Figs. S1, S2 reinforce the observed antiphase relationship, with *Acarinina* showing opposing patterns in the abundance distributions with respect to *Subbotina*. However, it is important to note that these changes in relative abundance are influenced by the closed-sum effect, where a decline in one genus leads to an apparent increase in others.

Among the minor genera, *Chiloguembelina* records the highest abundance in **Phase 1** such as *Igorina*, *Planorotalites*, and *Parasubbotina* (Fig. 4; Tables 2, S1). In **Phase 2**, *Subbotina senni* dominates, followed by *Igorina*, with minimal variability in *Parasubbotina*, *Planorotalites*, and *Catapsidrax*. Notably, *Chiloguembelina* and *Globanomalina* disappear at the start of Phase 2. The absence of the small-sized *Chiloguembelina* was confirmed by additional analysis of the ≥38 μm fraction. **Phase 3** records a decline in *S. senni*, accompanied by a slight increase in *Planorotalites*, *Pseudohastigerina*, and *Catapsidrax*. Throughout the three early Eocene phases, the genera *Planorotalites*, *Pseudohastigerina, Globanomalina, Catapsidrax*, and the species *Guembelitriodes nuttalli* remain rare in the assemblages, never exceeding together 10 % of the total planktic foraminifera abundance (Figs. 3,4; Tables 2, S1).

3.4. Variations in abundance of planktic foraminiferal taxa at Site U1510

Relative abundances of planktic foraminiferal genera display significant variations across the EECO at Site U1510 as well, especially in the genus *Morozovella* while *Acarinina* and *Subbotina* exhibit more stable trends for most of the studied interval (Figs. 6, 7; Tables S2, 3). Superimposed on these long-term trends are more abrupt, short-lived fluctuations in taxa abundance, often in concomitance with the main CIEs.

Cluster analysis based on the relative abundance of the dominant planktic foraminifera (*Morozovella*, *Acarinina*, and *Subbotina*) reveals

Table 2
Average relative abundance (%) of planktic foraminiferal genera across the three Phases identified in the cluster analysis at ODP Hole 762C (Fig. 3).

	Morozovella (%)	*Acarinina* (%)	*Subbotina* (%)	*S. senni* (%)	*Chiloguembelina* (%)	*Igorina* (%)	*Planorotalites* (%)	*Pseudohast* (%)	*Globorotaloides* (%)	*Paragloborotalia* (%)	*Parasubbotina* (%)	*Globoturborotalia* (%)	*Globanomalina* (%)	*Catapsidrax* (%)	*Guembelitrioides nuttalli* (%)
Max	36	81	62	12	25	12	6	7	1	0	6	1	2	6	1
Min	2	13	8	0	0	0	0	0	0	0	0	0	0	0	0
Average	13	41	32	2	4	3	1	1	0	0	2	0	0	1	0
Phase 3	12	28	41	1	9	4	2	0	0	0	3	0	0	1	0
Phase 2	14	57	19	4	0	3	0	1	0	0	1	0	0	1	0
Phase 1	16	28	46	1	0	2	1	2	0	0	1	0	0	3	0

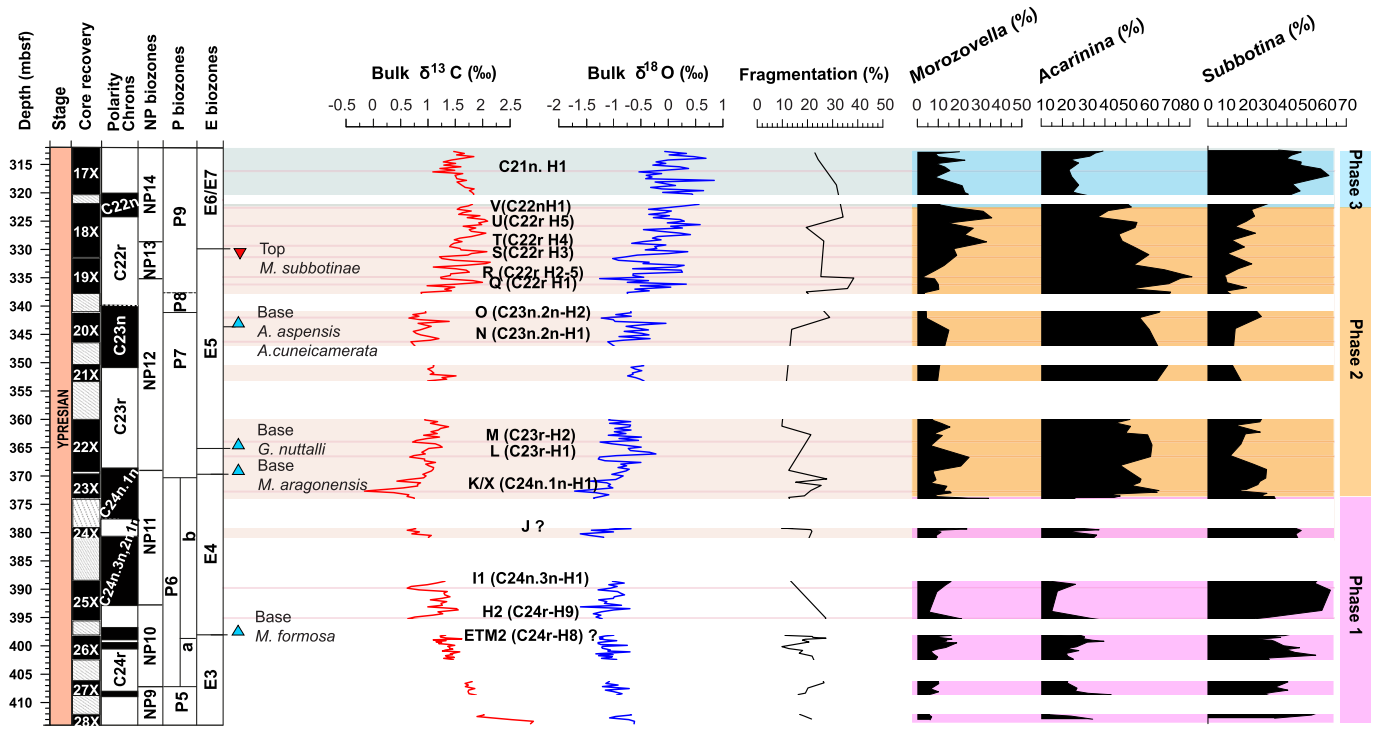

Fig. 3. Hole 762C: Bulk Carbon (red line) and Oxygen (Blue line) Stable Isotope curves plotted alongside Fragmentation Index (%) and relative abundances (%) of most abundant planktic foraminiferal genera, *Morozovella*, *Acarinina* and *Subbotina*. Depths are in mbsf according to Shipboard Scientific Party (1990), Magneto-stratigraphy follows Shamrock et al. (2012) and Xu et al. (2021), calcareous nannofossil biozonation is from Siesser and Bralower (NP biozones, 1992), planktic foraminifera zonation from Hancock et al. (2002) according to Berggren et al. (1995) (P biozones) and updated to Wade et al. (2011) zonal scheme, this study (E biozones). The main EECO CIEs identified are labelled according to Westerhold et al. (2017). The coloured bands identify the three main phases discussed in the text (Fig. 2). Pre-EECO and *J* CIE (pink, Phase 1), EECO (orange, Phase 2) and post-EECO (light blue, Phase 3) intervals. (For interpretation of the references to colour in this figure legend, the reader is referred to the web version of this article.)

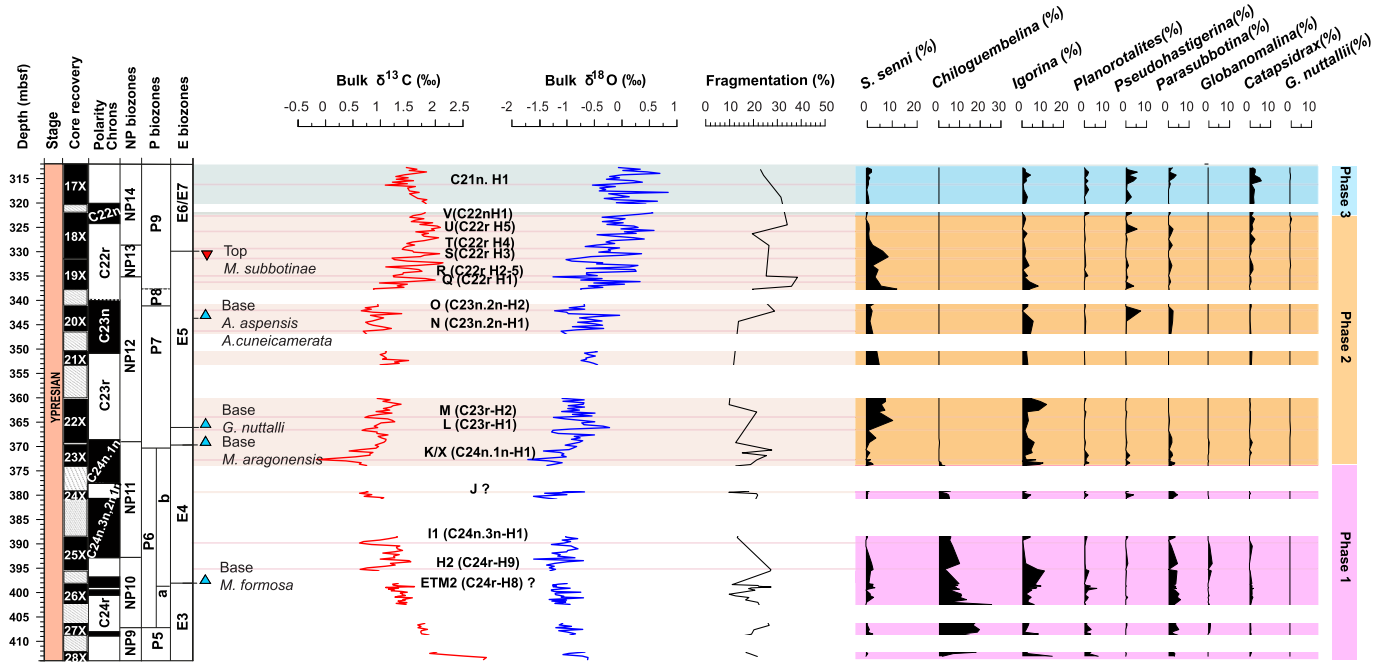

Fig. 4. Hole 762C. Relative abundances (%) of minor components of planktic foraminiferal assemblages: *Subbotina senni*, *Chiloguembelina, Igorina, Planorotalites, Pseudohastigerina, Parasubbotina, Globanomalina, Catapsidrax* and *Guembelittrioides nuttalli.* Other information is consistent with Fig. 3.

two distinct phases, Phase 1 and Phase 2, with Phase 1 subdivided in three subphases (a, b, c) ~~each~~ (Fig. 5): the EECO **Phase 1a** (violet), **1b** (blue) **1c** (light blue) and the late EECO **Phase 2.** The spatial separation of Phase 1 on the right side and Phase 2 on the center-left side in the NMDS analysis (Fig. 5 b) implies that the difference between the two groups is statistically significant. It is important to note that the

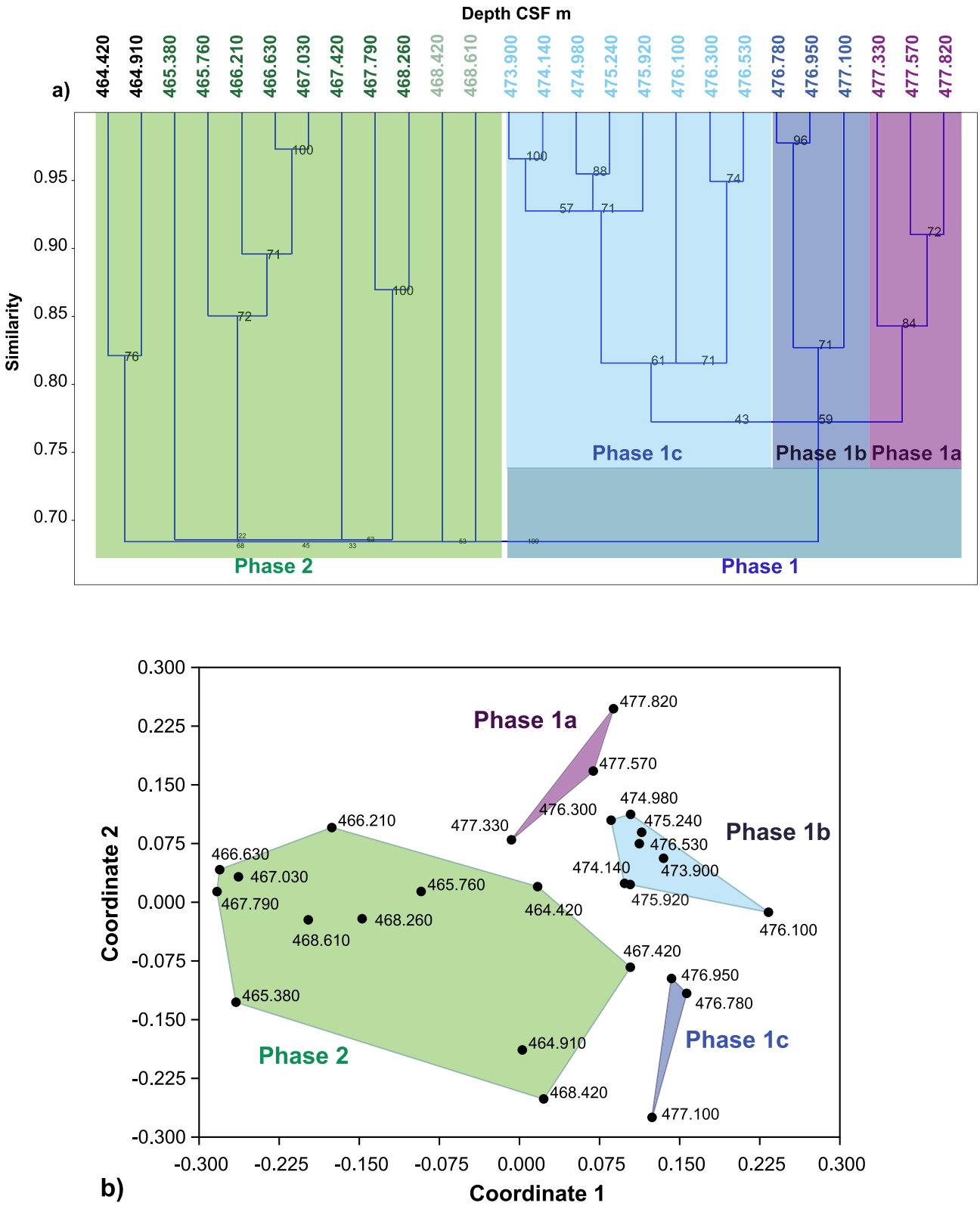

Fig. 5. a) Dendrogram of the stratigraphically-constrained multivariate classical clustering analysis performed on relative abundance (%) of planktic foraminiferal most abundant genera (*Morozovella, Acarinina* and *Subbotina*) across the studied interval at Site U1510, using a Paired Group (UPGMA) algorithm and the Bray-Curtis similarity index, with the main clusters named and highlighted as in Figs. 6, 7. Node values are for 1000 bootstraps. **b)** Clusters recovered by non-metric multi-dimensional scaling ordination analysis, using the Bray-Curtis similarity index, with hulls and labels representing groups recovered in Fig. 5a. Dots represents individual samples, with each dot corresponding to the phase it belongs to as identified in the dendrogram in Fig. 5a.

identified clusters at Site U1510 do not align perfectly with the CIEs. Additionally, the cluster colour scheme at Site U1510 does not follow that adopted for Site 762.

Phase 1 is characterized by the lowest abundances of *Morozovella*, while *Subbotina* and *Acarinina* fluctuate in the subphases. In **Phase 1a** (477.820–477.570 mbsf) *Acarinina* and *Morozovella* show very low abundances, while *Subbotina* reaches its highest abundance. In **Phase 1b** (477.330–476.950 mbsf) *Acarinina* dominates, recording its highest values, whereas *Subbotina* shows a temporary decline. *Morozovella* initially increases but declines throughout the rest of the phase. In **Phase 1c** (476.780–473.900 mbsf) *Acarinina* still dominates the assemblages followed by *Subbotina* with negligible variations. *Morozovella* exhibits a minor temporary increase, but its abundance never surpasses 6 % (Figs. 5, 6; Tables 3, S2).

In **Phase 2,** *Morozovella* markedly increases in abundance, while *Acarinina* shows a slight decline, and *Subbotina* maintains a generally stable trend. **Phase 2** is the largest and more spread-out cluster, indicating more variability within this phase compared to the tighter grouping in Phase 1 (Fig. 5 b). *Acarinina* continues to dominate but shows a decrease compared to the previous phase, while both *Morozovella* and *Subbotina* increase (Tables 3, S2; Figs. 5, 6).

Acarinina abundance often fluctuates in antiphase with *Morozovella* and *Subbotina*, particularly during the CIEs (Figs. S1, S2, Text S3). However, it is important to note that these changes in relative abundance are influenced by the closed-sum effect, where a decline in one genus leads to an apparent increase in others. As an example, the peak in *Acarinina* abundance at 372.67 mbsf during the K/X event might reflects a closed-sum effect, where this increase is accompanied by a short-term decline in *Subbotina* at the same depth. Similarly, at 334.91 mbsf, at the R event, the peak in *Acarinina* abundance is associated with a decline in both *Morozovella* and *Subbotina*.

Among the minor components of the assemblages, **Phase 1** is marked by a higher abundance of *Globanomalina*, followed by *Pseudohastigerina*, along with the disappearance of *Chiloguembelina* after the K/X CIE. In contrast, during **Phase 2**, both *Globanomalina* and *Pseudohastigerina* show a decrease in abundance, while *S. senni* experiences an increase. *Globanomalina* and *S. senni* are the more common genera of this group during this phase (Figs. 5, 7; Tables 3, S2).

EECO (violet, Phase 1), and upper EECO (green, Phase 2) intervals.

3.5. Planktic foraminiferal stable isotopes

Stable isotope carbon and oxygen data for the genera *Morozovella*, *Acarinina*, *Subbotina* and *Globanomalina* for the studied interval at Site U1510 are shown in Fig. 8a and Table S6.

The $\delta^{13}C$ values for *Morozovella*, *Acarinina*, and *Subbotina* show a decrease at the onset of the K/X Carbon Isotope Excursion (CIE) at 476.95 m CSF-A, followed by an increase towards higher values by the end of this CIE. At 474.98 m CSF-A, all genera exhibit $\delta^{13}C$ values slightly higher than their initial levels. However, *Morozovella* individuals were insufficient for isotope analysis at this depth, as were *Globanomalina* specimens during the K/X CIE. Throughout the studied interval, *Morozovella* consistently records slightly higher $\delta^{13}C$ values, followed by *Acarinina* and *Subbotina*, while *Globanomalina* generally shows the lowest values.

Acarinina and *Morozovella* exhibit the most negative $\delta^{18}O$ values recorded in this study (Fig. 8b, Table S6). Both genera show ~~a~~ slight minor negative values at the onset of the K/X transition. After this interval, the $\delta^{18}O$ values of the two genera appear more closed, approaching those of *Subbotina*. At 474.98 m CSF-A, *Acarinina* shows a slight increasing of recovery in $\delta^{18}O$ values whereas *Subbotina* records its less negative values, very close to *Globanomalina*.

4. Discussion

4.1. Impact of carbonate dissolution

To correctly interpret variations in the abundance of planktic foraminifera, it is essential to assess the potential effects of carbonate dissolution in deep-sea sediments, often associated with the rise of the CCD during hyperthermal events. A high F-index suggests carbonate dissolution, as this process breaks planktic foraminifera into fragments

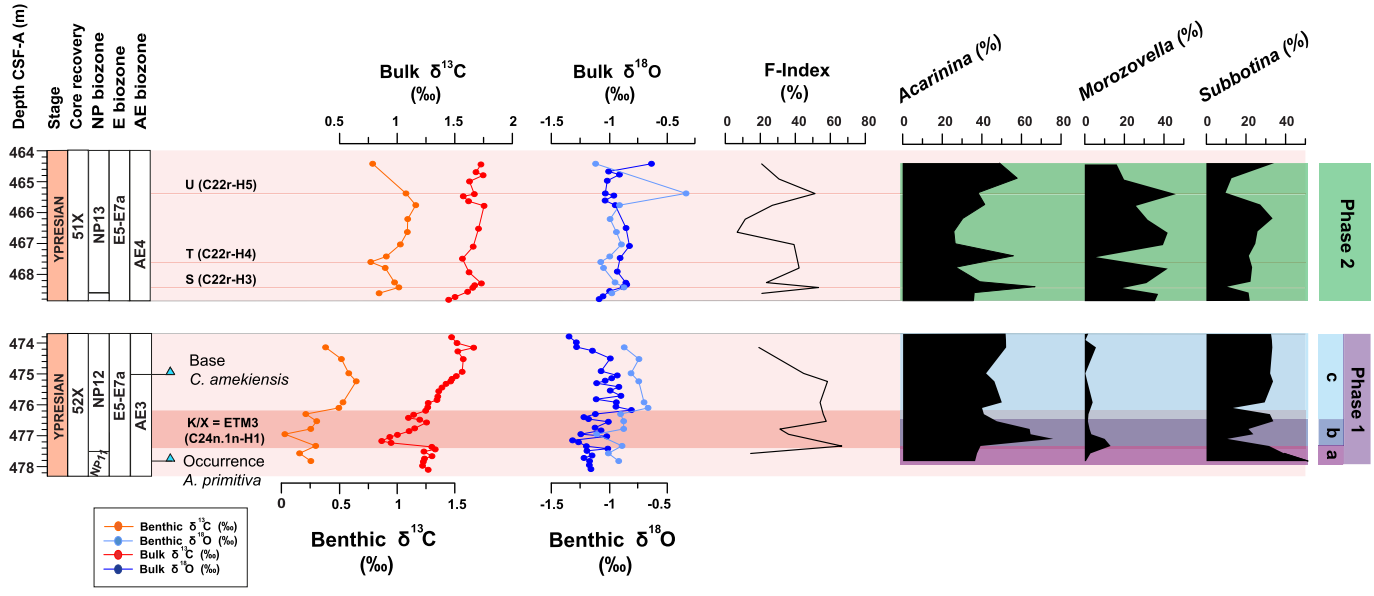

Fig. 6. Site 1510. Bulk $\delta^{13}C$ (orange curve), benthic $\delta^{13}C$ (red curve), bulk $\delta^{18}O$ (light blue curve) and benthic $\delta^{18}O$ (blue curve) from Alegret et al. (2021) plotted alongside Fragmentation Index (%) and relative abundances (%) of the most abundant planktic foraminifera genera *Morozovella*, *Acarinina* and *Subbotina*. Depths in Corrected Sea Floor (CSF/A m) and calcareous nannofossil zones are according to Alegret et al., 2021a, 2021bwho follow the zonation by Martini (1971) (NP biozones). Planktic foraminifera zonation from this study according to Wade et al. (2011) zonal scheme (E biozones), modified as in Luciani and Giusberti (2014). The Antarctic zonation AE of Huber and Quillévéré (2005) is from this study. The main EECO CIEs identified according to Alegret et al. (2021a, 2021b) and labelled as in Westerhold et al. (2017). The coloured bands identify the two main phases discussed in the text (Fig. 5). Initial. (For interpretation of the references to colour in this figure legend, the reader is referred to the web version of this article.)

Table 3
Planktic foraminifera genera relative abundance (%) mean values across the six subphases identified in the cluster analysis at ODP Site U1510.

	Morozovella %	*Acarinina* %	*Subbotina*%	*S. senni* %	*Globanomalina* %	*Chiloguembelina* %	*Pseudohastigerina* %
Average	16	45	26	1	9	1	2
Max	46	76	51	9	35	9	15
Min	0.3	26	10	0	0	0	0
Phase 2	30	41	22	3	4	0	0
Phase 1	4	49	30	0	12	1	4
1c	2	46	30	0	15	1	6
1b	5	68	18	0	4	2	2
1a	5	38	41	0	14	2	0

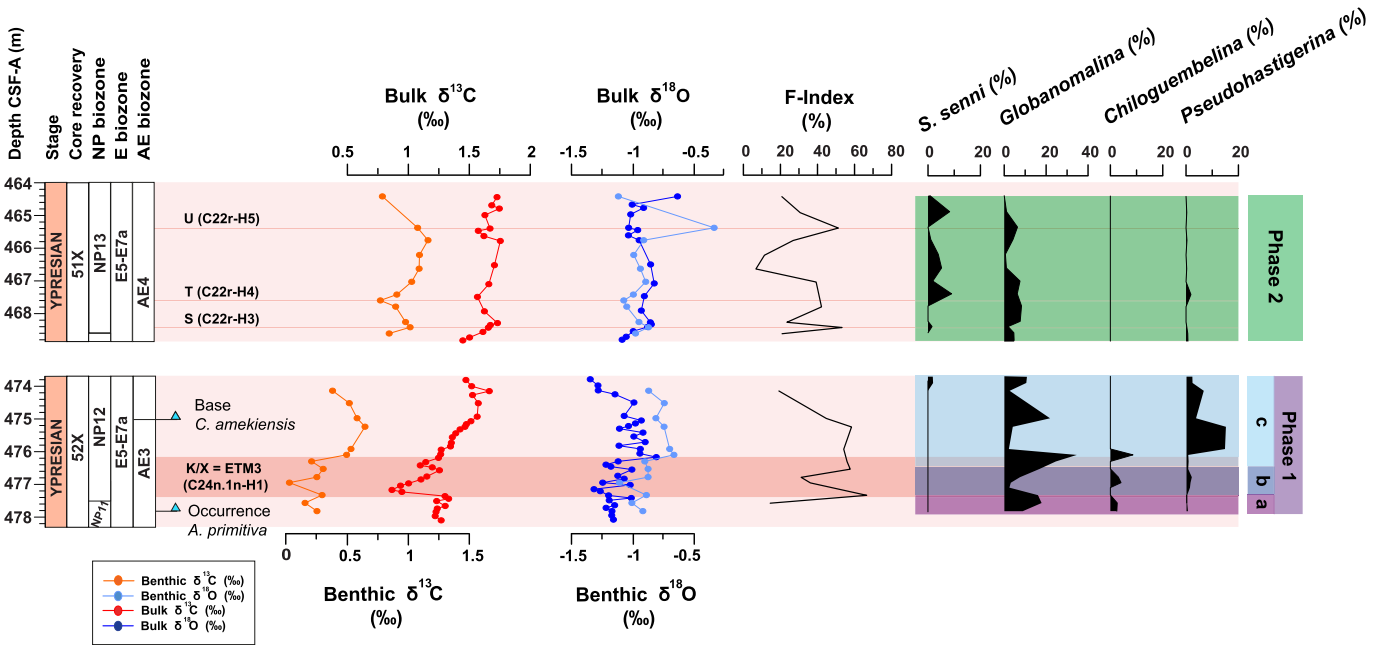

Fig. 7. Site U1510 Relative abundances (%) of minor component of planktic foraminiferal assemblages: *Subbotina senni, Globanomalina, Chiloguembelina, Pseudohastigerina.* Other information is consistent with Fig. 5.

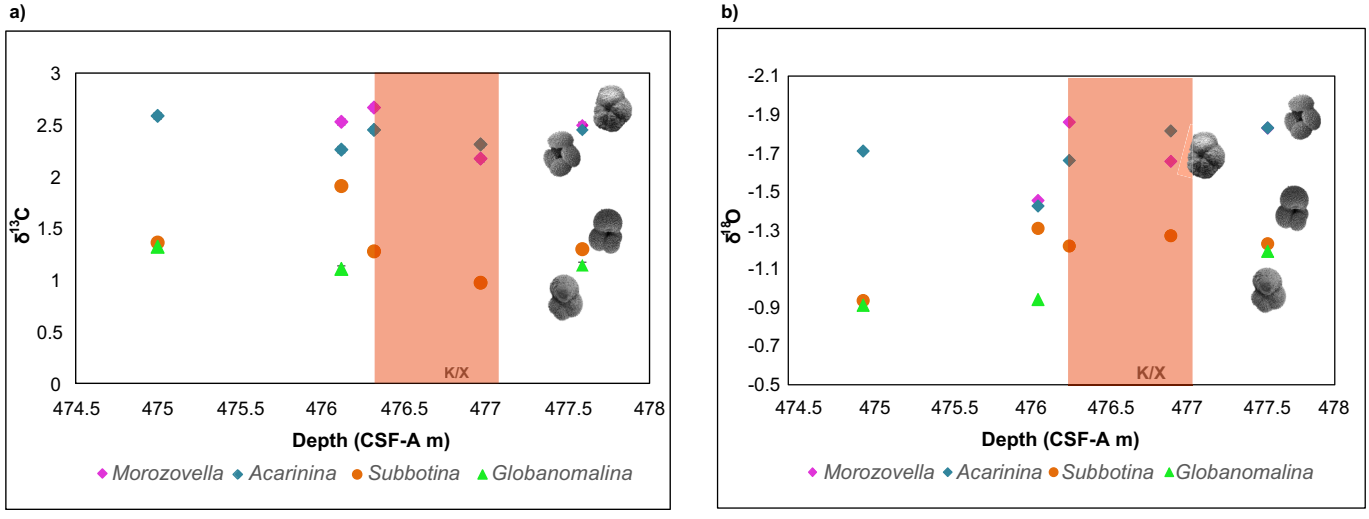

Fig. 8. a) $\delta^{13}C$ values for *Morozovella*, *Acarinina*, *Subbotina* and *Globanomalina* across the studied interval against Depths in CSF/A (m) according to Alegret et al. (2021). The K/X CIE is identified according to Alegret et al. (2021b) and following Westerhold et al. (2017). b) $\delta^{18}O$ values for *Morozovella*, *Acarinina*, *Subbotina* and *Globanomalina* across the studied interval against Depths in CSF/A (m) according to Alegret et al. (2021b). The K/X CIE is identified according to Alegret et al. (2021b) and following Westerhold et al. (2017).

(Berger, 1970; Hancock and Dickens, 2005). Studies of sediments from the latest Paleocene to early Eocene suggest some genera are more resistant than others to dissolution, with *Acarinina* being more resistant than *Morozovella*, and *Morozovella* than subbotinids (Petrizzo et al., 2008; Nguyen et al., 2009, 2011).

At Hole 762C and Site 1510, the mean fragmentation value is relatively low (21 % and 37 % respectively) suggesting that the structure of planktic foraminiferal assemblages was not significantly altered and its changes can be considered as reflecting primary variations. In addition, data from benthic foraminifera in Alegret et al. (2021b) confirm no significant $CaCO_3$-dissolution at the seafloor during the K/X. However, the F-index increases across most of the CIEs at both sites, although these increases are not proportional to CIE magnitudes, and variability in the F-index do not always correspond to hyperthermal events We cannot exclude that some of this variability might be related to sample treatment during laboratory procedures. The F-index increases at Hole 762C in Phase 2 (R event), and during Phase 2 at Site U1510, correspond to a peak in *Acarinina* and a decline in *Morozovella* and *Subbotina*. If changes in carbonate preservation acted as primary driver of observed planktic foraminiferal assemblages, the dominance of *Acarinina* during multiple CIEs could represent a taphonomic artifact. However, high abundances of *Acarinina* also occur during intervals with low F-index values, such as across Phase 2 at Hole 762C and the K/X CIE at Site U1510. This observation aligns with data from other locations where CIEs are associated with low F-index values and significant increases in *Acarinina* (Luciani et al., 2016; D'Onofrio et al., 2020; Filippi et al., 2024). Although there might be evidence of some carbonate dissolution in the water column or at the seafloor at the studied sites, it is probable that this process primarily enhanced pre-existing shifts in planktic foraminiferal assemblages rather than driving them directly.

4.2. Planktic foraminiferal paleoecology at Site U1510

Our stable isotope analysis on EECO planktic foraminiferal taxa from Site U1510 reveals evidence on their paleoecology and on the upper water stratification.

Morozovella and *Acarinina* were symbiont-bearing genera inhabiting the mixed layer, as inferred by their higher $\delta^{13}C$ values compared to deeper water dwellers (e.g., Pearson et al., 1993, 2006; Luciani et al., 2017a, Luciani et al., 2020a, 2020b; Davis et al., 2022; Filippi et al. unpublished results). At Site U1510, *Morozovella* and *Acarinina* display the highest $\delta^{13}C$ values compared to *Subbotina* (Fig. 8) thus confirming a shallow water habitat for the former genera and a deeper depth for the latter genus, as recorded previously (Fig. 9) (e.g., Dutton et al., 2005; Pearson et al., 2006; Luciani et al., 2017a, Luciani et al., 2020a, 2020b; Davis et al., 2022; Filippi et al., unpublished results).

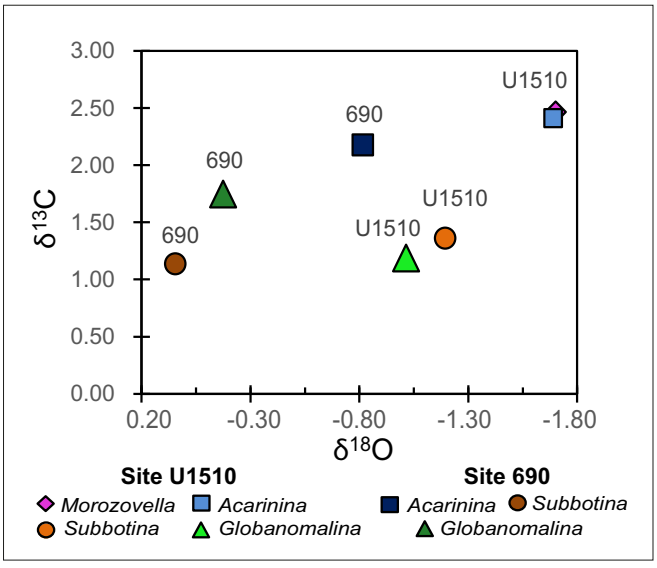

Fig. 9. Average $\delta^{13}C$ and $\delta^{18}O$ values for *Morozovella*, *Acarinina*, *Subbotina* and *Globanomalina* after the EECO onset at Site U1510, this study, compared to southern Atlantic locations data from Site 690 (Luciani et al., 2020).

The widespread warmest sustained temperatures at the EECO resulted in reduced latitudinal (Pross et al., 2012; Evans et al., 2018; Wilson et al., 2018) and lowered surface-to-deep temperature gradients as compared to modern ocean (e.g., (Huber and Caballero, 2011). The early Eocene was also characterized by a pelagic ecosystem that was concentrated in a relatively restricted depth range close to the ocean surface (Crichton et al., 2023) that reflects in relatively close $\delta^{13}C$ and $\delta^{18}O$ values recorded by mixed layer and deeper dweller taxa.

The differences between these two groups at Site U1510 account for ~1 ‰ in $\delta^{13}C$ values which is similar at Site 690 (Luciani et al., 2020a, 2020b) (Fig. 9). Interestingly, the analysis of planktic foraminiferal species at the tropical Atlantic Site 1051 below the EECO displays a major difference in $\delta^{13}C$ values of ~2 ‰ from shallow and deeper dwellers that then reduced up to ~0,5 ‰ within the EECO (Luciani et al., 2017a). After the EECO, the 'glassy' specimens examined from the Tanzania site shows a recovery of the difference of ~2 ‰ values between surface and deeper dwellers (Pearson et al., 2001). This pattern reinforces the evidence of restricted planktic foraminiferal depth range close to the ocean surface across the EECO and increase in the vertical mixing of the upper oceans (e.g., Hilting et al., 2008). The subsequent post-EECO cooling trend favored the establishment of new ecological niches resulting in planktic foraminiferal diversification (e.g., Fraass et al., 2015).

The early Eocene paleoecology of *Globanomalina* is still uncertain as some studies suggest it inhabited a shallow habitat (Pearson et al., 2006), while others, such as Luciani et al. (2020a, 2020b), propose a deeper habitat for *Globanomalina planoconica* at the southern Site 690 (Maud Rise), close to *Subbotina*. Our record shows lower $\delta^{13}C$ values for *Globanomalina* closer to those of *Subbotina,* consistent with Site 690 data (Fig. 9; Luciani et al., 2020a, 2020b) thus validating a deeper habitat,

Although typically considered a shallow-water species (Birch et al., 2012), the paleoecology of *Pseudohastigerina* is still unclear (Poore and Matthews, 1984; Boersma et al., 1987; Pearson et al., 2001; Keller et al., 1992; Sexton et al., 2006), suggesting this genus may have changed its habitat through time and space, so the ecological competition between *Pseudohastigerina* and *Globanomalina* remains uncertain.

4.3. Planktic foraminiferal response to the EECO at southern high latitudes and global resilience/vulnerability over space and time

At the investigated mid-to-high southern latitude sites, a lower mean abundance of *Morozovella* compared to *Acarinina* is expected, as *Morozovella* typically thrives in warm tropical settings, while *Acarinina* is also found at higher latitudes (Boersma et al., 1987; Premoli Silva and Boersma, 1988; Luciani et al., 2017a, 2017b; D'Onofrio et al., 2020). Before the EECO, *Morozovella* was indeed more abundant in warm low-latitude Atlantic and Pacific sites 1051 (around 40 %) (Luciani et al., 2017a; D'Onofrio et al., 2020; Filippi et al., 2024), followed by temperate southern Atlantic Site 1263 (24 %; Luciani et al., 2017b) and southern Pacific Hole 762C (16 %) (Fig. 10). The dominant *Morozovella* species at the studied sites are *M. crater* and *M. aragonensis*, with the former species being more abundant across the EECO at tropical -temperate (sites 1051 and 1263) and the latter taxon in the equatorial Atlantic (Site 1051) (D'Onofrio et al., 2020).

One of the main results of our analysis is the relatively stable abundance of the genus *Morozovella* at Hole 762C and its increase in the upper part of the Phase 2, from S to V events. The record of the EECO begins at the K/X event and does not include the J event (EECO beginning). Nevertheless, a marked *Morozovella* increase in abundance is evident also in this site from the same stratigraphic level (Figs. 3,6). Conversely, *Acarinina* is the dominant genus at both sites across the

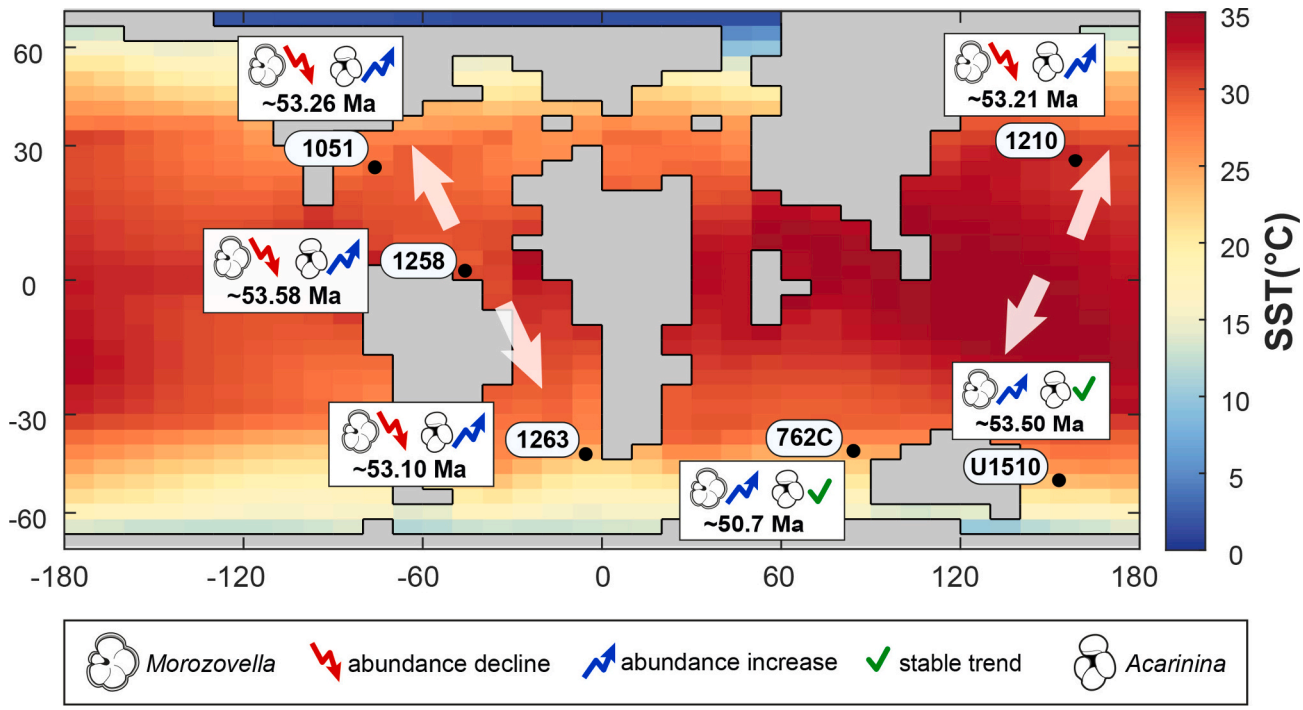

Fig. 10. Paleo-locations of ODP Sites from Indian Ocean Hole 762C and southern Pacific U1510 (this study), and tropical Pacific 1210 (Filippi et al., 2024), Atlantic 1051 (Luciani et al., 2017a), 1258 (D'Onofrio et al., 2020) and 1263 (Luciani et al., 2017b) showing the age (Ma) of the *Morozovella* decline in abundance, and *Acarinina* dominance. Drop, increase, or generally stable abundance are indicated by red descending arrows, blue ascending arrow, and green check mark, respectively. Sea surface temperature (SST) output is modelled by ForamEcoGEnIE modified from Filippi et al. (2024) and is a steady state early Eocene spin-up (Wilson et al., 2018). The white arrow is to note that the observed decline in *Morozovella* abundance originated in the Atlantic equatorial location and then occurred at temperate latitudes. (For interpretation of the references to colour in this figure legend, the reader is referred to the web version of this article.)

EECO, with pronounced peaks in abundance across the EECO hyperthermals at Hole 762C (Fig. 3) and during the events K/X, S, T, at Site U1510 (Fig. 6), thus attesting its tolerance to extreme warmth. Our record of *Acarinina* indicates that this genus, besides benefitting from increased temperature, was highly adaptable to varying nutrient levels, thriving in both oligotrophic conditions, as those at Hole 762C (e.g., Shamrock et al., 2012; Müller et al., 2019), and during intervals of increased nutrient availability such as at Site U1510 (Alegret et al., 2021a, 2021b).

Different from the significant changes experienced by *Morozovella* and *Acarinina*, the genus *Subbotina* displays moderate variations. *Subbotina* is considered a cold-water eutrophic index, typically dwelling deeper than the warmer surface waters preferred by *Acarinina* and *Morozovella* (e.g., Pearson et al., 2006 and references therein). Rising temperature in the *Subbotina* habitat may account for its decline close to hyperthermal events (Figs. 2, 5). However, some discrepancies emerge between the responses at the two sites. At Site U1510, *Subbotina* shows a long-term stable trend, while at Hole 762C, it registers a more evident decline during Phase 2 that may primarily derive from different nutrient availability at the two oceanographic settings, with Site U1510 recording more eutrophic conditions than Hole 762C (Shamrock et al., 2012; Müller et al., 2019; Alegret et al., 2021b). The establishment of cooler conditions after the EECO favored the cold index *Subbotina* which significantly increased in abundance whereas the warm indices *Acarinina* and *Morozovella* declined (Phase 3, Fig. 2).

Based on our new data on *Globanomalina*, we interpret the variations in abundance of this deeper dweller taxon recorded at Site U1510 as related to both temperature and trophic variations at its habitat. The marked drop in *Globanomalina* abundance at the K/X event (Phase 1b) may have resulted from the pronounced warming coupled with reduced food supply at depth. Alegret et al. (2021a, 2021b) document decoupled responses of calcareous nannofossils and benthic foraminifera across the K/X event, indicating enhanced eutrophication in surface waters without clear impacts at the seafloor, where oligo-mesotrophic conditions are suggested. Following this interpretation, we hypothesize that nutrients were primarily consumed in the mixed layers with limited input reaching the deeper waters and sea floor. In addition, *Globanomalina* may have suffered the K/X warming (Fig. 7). The abundance decrease of this genus observed above the K/X event (Phase 1) is, however, difficult to interpret. The correspondence of inverse abundance with *Pseudohastigerina* could suggest an ecological competition Although the ecology of *Pseudohastigerina* is still uncertain (Poore and Matthews, 1984; Boersma et al., 1987; Keller et al., 1992; Pearson et al., 2001; Sexton et al., 2006; Birch et al., 2012).

Interestingly, our record from southern mid-to-high latitudes does not record the marked demise of *Morozovella* at the EECO beginning as observed in Atlantic and tropical Pacific locations (Luciani et al., 2016, 2017a, 2017b; D'Onofrio et al., 2020; Filippi et al., 2024).

The subsequent increase in *Morozovella* abundance during the late EECO interval at Hole 762C and Site U1510 (Figs. 2, 5) might reflect a southern migration (Fig. 10). Poleward migrations have been observed as the response of plankton communities to past global warming events (e.g, Thomas, 2007; Bown and Pearson, 2009; Speijer et al., 2012; D'Onofrio et al., 2020; Woodhouse et al., 2021; Barrett et al., 2023). In addition, D'Onofrio et al. (2020) and Filippi et al. (2024) highlight that the decline in *Morozovella* abundance recorded at the EECO beginning started first at equatorial latitudes and later at tropical and temperate ones. This evidence has been interpreted as a migration over ~500 kyr to cooler latitudes to escape the effects of warming (D'Onofrio et al., 2020; Filippi et al., 2024). Swain et al. (2024) also support the hypothesis that that higher latitudes of the Southern Hemisphere may have acted as ecological refugia during peak Cenozoic warmth. However, the supposed *Morozovella* migration, took approximately 2 Myr, as derived from the timing of their decline at lower latitudes to their abundance increase at our sites in the late EECO, a time interval much longer than the estimated 500 kyr estimated to move from equatorial to temperate

regions (D'Onofrio et al., 2020; Filippi et al., 2024). Nevertheless, while high-latitude sites possibly provided a refuge from the extreme heat of equatorial regions, these environments were still suboptimal for *Morozovella*, which was unable to dominate the assemblages.

In contrast, *Acarinina* emerged as the most adaptable genus during the EECO, thriving across a range of latitudes and environments (Luciani et al., 2016, 2017a, 2017b; D'Onofrio et al., 2020; Filippi et al., 2024).

Although inferences of changes in paleoecology should derive from species-specific we attempt a speculation based on our stable isotope analysis at genus level to get insights on the widespread *Acarinina* dominance across the EECO. The slightly minor $\delta^{13}C$ values exhibited in this study by *Acarinina* as compared to *Morozovella* across the K/X CIE (Fig. 8a) might indicate that this genus could have been able to change/reduce its photosymbiosis relationship moving deeper in the mixed layer in response to temperature peak and nutrient fluctuations. Interestingly, the tropical Pacific sites 1209–1210 record the same differences in the EECO interval (Davis et al., 2022; Filippi et al., unpublished results. These data from Pacific Ocean were collected both at genus level and on species that are different from those dominating at our southern sites. This may indicate that the constantly slightly minor $\delta^{13}C$ values displayed by *Acarinina* are beyond the limits deriving from the measured species or different proportions of examined species over space and time and may indeed signify differences in ecological behaviour.

The *Acarinina* ecological versatility allowed it to dominate across such a range of environmental conditions positively responding to both temperature and nutrient fluctuations thus explaining its dominance during the EECO (Luciani et al., 2016, 2017a, 2017b; D'Onofrio et al., 2020; Filippi et al., 2024, Filippi et al., unpublished results).

4.4. *Chiloguembelina 'eclipse' across the EECO*

The genus *Chiloguembelina*, ranging from the lower Danian to the middle Oligocene (e.g., Pearson et al., 2006), is known for its abrupt decline persisting across the EECO from the K/X Event (52.86 Ma) in the Atlantic and tropical Pacific oceans (Luciani et al., 2020a, 2020b; Filippi et al., 2024). We document that this genus shows a similar 'eclipse' at Hole 762C and Site U1510 in the same stratigraphic level. This genus is absent even in intervals where the dissolution proxy F-index is very low, thus excluding taphonomic bias (Figs. 4, 7). In addition, their presence was not overlooked in our analysis of the $\geq$63 μm fraction because the observation of the portions between 38 μm and 63 μm confirms the absence of this small-sized genus from the K/X event.

Some studies suggest that the biserial *Chiloguembelina* were low-oxygen tolerant thriving in the Oxygen Depleted Zone (ODZ), meso- to eutrophic thermocline dwellers (e.g., Boersma and Premoli Silva, 1989). Conversely, other Cenozoic records indicate that this genus may have inhabited surface waters (e.g., Barrera and Huber, 1991; D'haenens et al., 2012; Fucek et al., 2018). $\delta^{13}C$ data from the Atlantic Ocean during the EECO (Luciani et al., 2020a, 2020b) support the view that *Chiloguembelina* shared the deep water habitat of subbotinids. Hence, the decline of *Chiloguembelina* could have been influenced by a reduction in nutrient supply to deeper waters and/or a contraction of the Oxygen Minimum Zone (OMZ) (Luciani et al., 2020a, 2020b). The EECO ODZ contraction has been reconstructed through foraminiferal bound nitrogen isotopes in the Atlantic and tropical Pacific (Auderset et al., 2022). Elevated ocean temperatures enhanced the rate of bacterial respiration and remineralization significantly resulting in more efficient recycling of carbon and nutrients higher in the water column as demonstrated by early Eocene $\delta^{13}C_{DIC}$ depth profiles that are sharper than modern gradients consistent with shallower remineralization (Olivarez Lyle and Lyle, 2006; Hilting et al., 2008; John et al., 2013, 2014). Hence, the early Eocene conditions may have exacerbated a reduced availability of nutrients in the deeper waters (Crichton et al., 2023). However, subbotinids, largely sharing the *Chiloguembelina* habitat, were not markedly impacted because subbotinids only moderately decrease in abundance but do not 'disappear'. Therefore, the triggering causes of the chiloguembelinids eclipse at the EECO appear to be primarily related to the improved water oxygen content. This evidence, supported by the foraminiferal bound nitrogen record (Auderset et al., 2022) conflicts with the supposition of shoaling and intensification of the ODZ during ocean warming (e.g., Crichton et al., 2023) and requires enhanced comprehension of paleocenographic mechanisms during global warmings. The genus *Chiloguembelina* did not recover above the EECO at the sites investigated (Phase 3 of Fig. 4), suggesting a still contracted ODZ and/or that *Subbotina* preferentially exploited the food availability in the deeper water column.

The observed virtual disappearance of *Chiloguembelina* from the K/X event at Hole 762C and Site U1510 underlines that this pattern is likely global, being also detected in both Atlantic and Pacific oceans (Luciani et al., 2020a; Filippi et al., 2024) and may represent an additional useful biostratigraphic tool.

In conclusions, the record of the planktic foraminiferal genera during the EECO across different oceanic regions provides a compelling narrative of how these species adapted—or struggled— in response to changing temperature and nutrient availability. Following the resilience definition (Capdevila et al., 2020; Hodgson et al., 2015), planktic foraminiferal communities proved to be not resilient in all the Atlantic, Pacific and Southern Oceans sites, as recording permanent changes across the EECO without returning to the previous stable state.

5. Conclusions

This study provides new insights into the responses of planktic foraminiferal communities to environmental changes during the Early Eocene Climatic Optimum (EECO) at mid-to-high-latitude Site U1510 and Hole 762C.

Our findings confirm the global dominance of the mixed layer genus *Acarinina* across the EECO. The ecological versatility and adaptability of this genus made it able to benefit of the increased temperatures and to thrive in both oligotrophic and eutrophic conditions during the EECO.

Unlike the dramatic decline of *Morozovella* observed in equatorial and tropical regions we record increased abundance in the late EECO at mid-to-high-latitudes that allowed this genus to escape from the extreme heat experienced in tropical areas.

The abundance reduction across the EECO of the cold-index *Subbotina* at Hole 762C appears as a response to the temperature increase and food reduction in deeper waters. The absence of a decline at Site U1510 may be attributed to greater food availability, reinforcing the importance of the distinct oceanic influences in shaping foraminiferal communities during this interval.

Our new data from Site U1510 on *Globanomalina* stable isotope paleoecology, so far uncertain, reveal a deep-water habitat. The observed variations in *Globanomalina* abundance, particularly the significant decline at the K/X event, appear to correlate with warming and reduced food supply in deep water.

The permanent disappearance of the genus *Chiloguembelina* at Hole 762C and Site U1510, starting at the K/X Event, reflects a larger scale, possibly global pattern, as it has been also observed in the Atlantic and tropical Pacific oceans from the same level. This might be primarily attributed to ODZ contraction.

The reconstruction of biogeographic patterns of planktic foraminifera across the EECO from different oceans and latitudinal settings reveals significant scenarios that may be useful to evaluate the consequences of future climate change. Changes occurred underlying the critical role of temperature, nutrient availability, and oxygenation in shaping the evolutionary and abundance shapes of these key marine calcifiers microorganisms. Taxa able to adapt to the variations of these aspects, such as *Acarinina* gained success whereas the *Morozovella* and *Chiloguembelina* minor ecological plasticity led to their decline. In all the Atlantic, Pacific and Southern Oceans sites, planktic foraminiferal communities proved to be not resilient as moving to a different configuration across the EECO and never returning to the previous stable state.

CRediT authorship contribution statement

Giulia Filippi: Writing – review & editing, Writing – original draft, Visualization, Validation, Software, Resources, Methodology, Investigation, Formal analysis, Data curation, Conceptualization. **Valeria Luciani:** Writing – review & editing, Writing – original draft, Visualization, Validation, Supervision, Resources, Project administration, Methodology, Investigation, Funding acquisition, Formal analysis, Conceptualization.

Declaration of competing interest

The authors declare that they have no known competing financial interests or personal relationships that could have appeared to influence the work reported in this paper.

Data availability

Data are available on the Supporting Information related to this Manuscript and will be available with the pubblication

Acknowledgments

We are deeply grateful to the reviewers F. Boscolo-Galazzo, A. Woodhouse, and the Guest Editor L. Angiolini for their detailed and insightful revisions, which have significantly improved this study. The samples used in this research were provided by the Ocean Drilling Program, and we thank the Bremen Core Repository for handling the sample requests. Sincere thanks go to C. Agnini and V. Brombin, for performing stable isotope analysis at the University of Padua and Ferrara, Italy.

This work has been funded to VL and G.F. by MIUR, Italy, PRIN 2017 "Biota resilience to global change: biomineralization of planktic and benthic calcifiers in the past, present and future" (grant: 80007370382) and FAR 2023 (University of Ferrara).

Appendix A. Supplementary data

Supplementary data for this article can be found online at [URL] and include Tables S1-S6, which detail planktic foraminiferal relative abundances, stable isotopes, fragmentation index and depth for Hole 762C and U1510. Supplementary data to this article can be found online at https://doi.org/10.1016/j.palaeo.2024.112660.

References

Agnini, C., Macrì, P., Backman, J., Brinkhuis, H., Fornaciari, E., Giusberti, L., Luciani, V., Rio, D., Sluijs, A., Speranza, F., 2009. An early Eocene carbon cycle perturbation at ~52.5 Ma in the Southern Alps: Chronology and biotic response. Paleoceanography 24. https://doi.org/10.1029/2008PA001649.

Alegret, L., Arreguín-Rodríguez, G.J., Trasviña-Moreno, C.A., Thomas, E., 2021a. Turnover and stability in the deep sea: Benthic foraminifera as tracers of Paleogene global change. Glob. Planet. Chan. 196, 103372. https://doi.org/10.1016/j.gloplacha.2020.103372.

Alegret, L., Harper, D.T., Agnini, C., Newsam, C., Westerhold, T., Cramwinckel, M.J., Dallanave, E., Dickens, G.R., Sutherland, R., 2021b. Biotic Response to Early Eocene Warming events: Integrated Record from Offshore Zealandia, North Tasman Sea. Paleoceanogr. Paleoclimatology 36. https://doi.org/10.1029/2020PA004179 e2020PA004179.

Anagnostou, E., John, E.H., Babila, T.L., Sexton, P.F., Ridgwell, A., Lunt, D.J., Pearson, P. N., Chalk, T.B., Pancost, R.D., Foster, G.L., 2020. Proxy evidence for state-dependence of climate sensitivity in the Eocene greenhouse. Nat. Commun. 11, 4436. https://doi.org/10.1038/s41467-020-17887-x.

Auderset, A., Moretti, S., Taphorn, B., Ebner, P.-R., Kast, E., Wang, X.T., Schiebel, R., Sigman, D.M., Haug, G.H., Martínez-García, A., 2022. Enhanced Ocean oxygenation during Cenozoic warm periods. Nature 609, 77–82.

Aze, T., Ezard, T.H.G., Purvis, A., Coxall, H.K., Stewart, D.R.M., Wade, B.S., Pearson, P. N., 2011. A phylogeny of Cenozoic macroperforate planktonic foraminifera from fossil data. Biol. Rev. 86, 900–927. https://doi.org/10.1111/j.1469-185X.2011.00178.x.

Banner, F.T., Blow, W.H., 1959. The classification and stratigraphical distribution of the Globigerinacea. Palaeontology 2, 1–27.

Barrera, E., Huber, B.T., 1991. Paleogene and early Neogene oceanography of the southern Indian Ocean: Leg 119 foraminifer stable isotope results. In: Barron, J., Larsen, B., et al. (Eds.), Proc. ODP, Sci. Results, 119: College Station, TX (Oc. Drill. Prog.), pp. 693–717. https://doi.org/10.2973/odp.proc.sr.119.167.1991.

Barrett, R., Adebowale, M., Birch, H., Wilson, J.D., Schmidt, D.N., 2023. Planktic foraminiferal resilience to environmental change associated with the PETM. Paleoceanogr. Paleoclimatology 38. https://doi.org/10.1029/2022PA004534 e2022PA004534.

Beckmann, J.P., 1953. Die foraminiferen der Oceanic Formation (Eocaen-Oligocaen) von Barbados. In: Kleine Antillen: Eclogae Geologicae Helvetiae, 46, pp. 301–412.

Berger, W.H., 1970. Planktonic Foraminifera: Selective solution and the lysocline. Mar. Geol. 8, 111–138. https://doi.org/10.1016/0025-3227(70)90001-0.

Berggren, W.A., Kent, D.V., Swisher, I., Carl, C., Aubry, M.P., 1995. A Revised Cenozoic Geochronology and Chronostratigraphy. In: Geochronology, Time Scales and Global Stratigraphic Correlation. SEPM Society for Sedimentary Geology. https://doi.org/10.2110/pec.95.04.0129.

Bijl, P.K., Bendle, J.A.P., Bohaty, S.M., Pross, J., Schouten, S., Tauxe, L., Stickley, C.E., McKay, R.M., Röhl, U., Olney, M., Sluijs, A., Escutia, C., Brinkhuis, H., Scientists, E. 318, Klaus, A., Fehr, A., Williams, T., Carr, S.A., Dunbar, R.B., Gonzàlez, J.J., Hayden, T.G., Iwai, M., Jimenez-Espejo, F.J., Katsuki, K., Kong, G.S., Nakai, M., Passchier, S., Pekar, S.F., Riesselman, C., Sakai, T., Shrivastava, P.K., Sugisaki, S., Tuo, S., Flierdt, T., Welsh, K., Yamane, M., 2013. Eocene cooling linked to early flow across the Tasmanian Gateway. Proc. Natl. Acad. Sci. 110, 9645–9650. https://doi.org/10.1073/pnas.1220872110.

Birch, H.S., Coxall, H.K., Pearson, P.N., 2012. Evolutionary ecology of Early Paleocene planktonic foraminifera: size, depth habitat and symbiosis. Paleobiol 38 (3), 374–390.

Boersma, A., Silva, I.P., Shackleton, N.J., 1987. Atlantic Eocene planktonic foraminiferal paleohydrographic indicators and stable isotope paleoceanography. Paleoceanography 2, 287–331. https://doi.org/10.1029/PA002i003p00287.

Bolli, H.M., 1957. Planktonic foraminifera from the Eocene Navet and San Fernando formations of Trinidad, B.W.I. In: Loeblich,A. R., Jr., and collaborators, Studies in Foraminifera: Unit. States Natl. Museum Bull, 215, pp. 155–172.

Bown, P., Pearson, P., 2009. Calcareous plankton evolution and the Paleocene/Eocene thermal maximum event: New evidence from Tanzania. Mar. Micropaleontol. 71, 60–70. https://doi.org/10.1016/j.marmicro.2009.01.005.

Brotzen, F., Pozaryska, K., 1961. Foraminifères du Paléocène et de l'Eocène inférieur en Pologne septentrionale; remarques paléogéographiques. Rev. Micropaleontol. 4, 155–166.

Capdevila, P., Stott, I., Beger, M., Salguero-Gómez, R., 2020. Towards a comparative framework of demographic resilience. Trends in Ecology and Evolution 35 (9), 776–786. https://doi.org/10.1016/j.tree.2020.05.001.

Cenozoic CO2 Proxy Integration Project (CenCO2PIP) Consortium, 2023. Toward a Cenozoic history of atmospheric CO2. Science 382, eadi5177. https://doi.org/10.1126/science.adi5177.

Chaabane, S., Garidel, T., Meilland, J., Sulpis, O., Chalk, T., Brummer, G.-J., Mortyn, P. G., Giraud, X., Howa, H., Casajus, N., Kuroyanagi, A., Beaugrand, G., Schiebel, R., 2023. Modern planktonic Foraminifera: migrating is not enough. Biol. Sci. https://doi.org/10.21203/rs.3.rs-3485983/v1.

Cooley, S., Schoeman, D., Bopp, L., Boyd, P., Donner, S., Ito, S., Kiessling, W., Martinetto, P., Ojea, E., Racault, M.-F., Rost, B., Skern-Mauritzen, M., Ghebrehiwet, D.Y., Bell, J.D., Blanchard, J., Bolin, J., Cheung, W.W.L., Cisneros-Montemayor, A., Dupont, S., Dutkiewicz, S., Frölicher, T., Gaitán-Espitia, J.-D., Molinos, J.G., Gurney-Smith, H., Henson, S., Hidalgo, M., Holland, E., Kopp, R., Kordas, R., Kwiatkowski, L., Le Bris, N., Lluch-Cota, S.E., Logan, C., Mark, F.C., Mgaya, Y., Moloney, C., Muñoz Sevilla, N.P., Randin, G., Raja, N.B., Rajkaran, A., Richardson, A., Roe, S., Ruiz Diaz, R., Salili, D., Sallée, J.-B., Scales, K., Scobie, M., Simmons, C.T., Torres, O., Yool, A., 2022. Chapter 3: Oceans and Coastal Ecosystems and their Services. In Climate Change 2022: Impacts, Adaptation and Vulnerability. IPCC AR6 WGII. URL 379–550. https://www.ipcc.ch/report/ar6/wg2/downloads/report/IPCC_AR6_WGII_FinalDraft_Chapter03.pdf. accessed 9.9.24.

Cramer, B., Wright, J., Aubry, M.P., 2003. Orbital climate forcing of δ13C excursions in the late Paleocene–early Eocene (Chrons C24n–C25n). Paleoceanography 18, 1097. https://doi.org/10.1029/2003PA000909.

Crichton, K.A., Wilson, J.D., Ridgwell, A., Boscolo-Galazzo, F., John, E.H., Wade, B.S., Pearson, P.N., 2023. What the geological past can tell us about the future of the ocean's twilight zone. Nat. Commun. 14 (1), 2376. https://doi.org/10.1038/s41467-023-37781-6.

Crouch, E.M., Shepherd, C.L., Morgans, H.E.G., Naafs, B.D.A., Dallanave, E., Phillips, A., Hollis, C.J., Pancost, R.D., 2020. Climatic and environmental changes across the early Eocene climatic optimum at mid-Waipara River, Canterbury Basin, New Zealand. Earth-Science Reviews 200, 102961. https://doi.org/10.1016/j.earscirev.2019.102961.

Cushman, J.A., Renz, H.H., 1942. Eocene, Midway, Foraminifera from Soldado Rock, Trinidad: Contributions Cushman Lab. Foraminifer. Res. 18, 1–14.

Davidzon, R.M., 1976. Novyy paleogenovyy rod planktonnykh foraminifer: Trudy Vsesoyuznogo Nauchnoissledovatel'skogo Geologorazvedochnogo Neftyanogo Instituta (VNIGNI). Tadzhikskoe Otdelenie 183, 197–199.

Davis, C.V., Shaw, J.O., D'haenens, S., Thomas, E., Hull, P.M., 2022. Photosymbiont associations persisted in planktic foraminifera during early Eocene hyperthermals at Shatsky rise (Pacific Ocean). PloS One 17, e0267636. https://doi.org/10.1371/journal.pone.0267636.

D'haenens, S., Bornemann, A., Roose, K., Claeys, P., Speijer, R., 2012. Stable isotope paleoecology (δ13C and δ18O) of early Eocene Zeauvigerina aegyptiaca from the North Atlantic (DSDP Site 401). Austrian J. Earth Sci. 105 (1), 179–188.

D'Onofrio, R., Luciani, V., Dickens, G.R., Wade, B.S., Kirtland Turner, S., 2020. Demise of the planktic foraminifer genus Morozovella during the early Eocene Climatic Optimum: new records from ODP Site 1258 (Demerara rise, Western Equatorial Atlantic) and Site 1263 (Walvis Ridge, South Atlantic). Geosciences 10 (3). https://doi.org/10.3390/geosciences10030088. Article 3.

Dutton, A., Lohmann, K.C., Leckie, R.M., 2005. Insights from the Paleogene tropical Pacific: Foraminiferal stable isotope and elemental results from Site 1209, Shatsky Rise. Paleoceanography 20. https://doi.org/10.1029/2004PA001098.

Evans, D., Sagoo, N., Renema, W., Cotton, L.J., Müller, W., Todd, J.A., Saraswati, P.K., Stassen, P., Ziegler, M., Pearson, P.N., Valdes, P.J., Affek, H.P., 2018. Eocene greenhouse climate revealed by coupled clumped isotope-Mg/ca thermometry. Proc. Natl. Acad. Sci. 115 (6), 1174–1179. https://doi.org/10.1073/pnas.1714744115.

Filippi, G., Barrett, R., Schmidt, D.N., D'Onofrio, R., Westerhold, T., Brombin, V., Luciani, V., 2024. Impacts of the Early Eocene Climatic Optimum (EECO, ~53-49 Ma) on Planktic Foraminiferal Resilience. Paleoceanogr. Paleoclimatol. 39. https://doi.org/10.1029/2023PA004820 e2023PA004820.

Filippi, G., Sigismondi, S., Schmidt, D.N., Luciani, V., unpublished results. Contrasting Response in test size and abundance of Planktic Foraminifera Morozovella and Acarinina to the EECO in the Tropical Pacific Ocean.

Finkel, Z.V., Sebbo, J., Feist-Burkhardt, S., Irwin, A.J., Katz, M.E., Schofield, O.M.E., Young, J.R., Falkowski, P.G., 2007. A universal driver of macroevolutionary change in the size of marine foraminiferal 18O over the past 95 million years. Proc. National Academy Sci. 119. https://doi.org/10.1073/pnas.2111332119 e2111332119.

Fraass, A.J., Kelly, D.C., Peters, S.E., 2015. Macroevolutionary History of the Planktic Foraminifera. Ann. Rev. Earth Planet. Sci. 43, 139–166. https://doi.org/10.1146/annurev-earth-060614-105059.

Fucek, V.P., Kucenjak, M.H., Huber, B.T., 2018. Taxonomy, biostratigraphy, and phylogeny of Oligocene Chiloguembelina and Jenkinsina. Atlas of Oligocene Planktonic Foraminifera. In: Lawrence, 46. Cushman Foundation Spec. Publ, Kansas USA, pp. 459–480.

Gaskell, D.E., Huber, M., O'Brien, C.L., Inglis, G.N., Acosta, R.P., Poulsen, C.J., Hull, P. M., 2022. The latitudinal temperature gradient and its climate dependence as inferred from foraminiferal δ18O over the past 95 million years. Proc. Natl. Acad. Sci 119, e2111332119. https://doi.org/10.1073/pnas.2111332119.

Glaessner, M.F., 1937. Planktonische Foraminiferen aus der Kreide und dem Eozän und ihre stratigraphische Bedeutung: Studies in Micropaleontology. Publ. Lab. Paleontol, Moscow University 1, 27–52.

Green, O.R., 2001. A manual of practical laboratory and field techniques in palaeobiology, 538. Kluwer Academic.

Hamilton, E.L., 1953. Upper cretaceous, Tertiary and recent planktonic Foraminifera from mid-Pacific flat-topped seamounts. J. Paleo. 27, 207–237.

Hammer, Ø., Harper, D.A.T., Ryan, P.D., 2001. PAST: Paleontological statistics software package for education and data analysis. Palaeontol. Electr. 4 (1), 9pp.

Hancock, H., Dickens, G., 2005. Carbonate dissolution episodes in Paleocene and Eocene sediment, Shatsky rise, West-Central Pacific. Proc. ODP Sci. Res. 198, 1–24.

Hancock, H., Chaproniere, G., Dickens, G., Henderson, R., 2002. Early Palaeogene planktic foraminiferal and carbon isotope stratigraphy, Hole 762C, Exmouth Plateau, northwest Australian margin. J. Micropalaeontol. 21, 29–42. https://doi.org/10.1144/jm.21.1.29.

Haque, A.F.M.M., 1956. The Foraminifera of the Ranikot and the Laki of the Nammal Gorge, Salt Range: Pakistan Geological Survey. Paleontologia Pakistanica 1, 1–300.

Hilting, A.K., Kump, L.R., Bralower, T.J., 2008. Variations in the oceanic vertical carbon isotope gradient and their implications for the Paleocene-Eocene biological pump. Paleoceanography 23. https://doi.org/10.1029/2007PA001458.

Hines, B., Hollis, C., Atkins, C., Baker, J., Morgans, H., Strong, C., 2017. Reduction of oceanic temperature gradients in the early Eocene Southwest Pacific Ocean. Palaeogeogr. Palaeoclimatol. Palaeoecol. 475, 41–54. https://doi.org/10.1016/j.palaeo.2017.02.037.

Hodgson, D., McDonald, J.L., Hosken, D.J., 2015. What do you mean, 'resilient'? Trends in Ecology and Evolution 30 (9), 503–506. https://doi.org/10.1016/j.tree.2015.06.010.

Hollis, C.J., Handley, L., Crouch, E.M., Morgans, H.E.G., Baker, J.A., Creech, J., Collins, K.S., Gibbs, S.J., Huber, M., Schouten, S., Zachos, J.C., Pancost, R.D., 2009. Tropical Sea temperatures in the high-latitude South Pacific during the Eocene. Geology 37, 99–102. https://doi.org/10.1130/G25200A.1.

Hollis, C.J., Taylor, K.W.R., Handley, L., Pancost, R.D., Huber, M., Creech, J.B., Hines, B. R., Crouch, E.M., Morgans, H.E.G., Crampton, J.S., Gibbs, S., Pearson, P.N., Zachos, J.C., 2012. Early Paleogene temperature history of the Southwest Pacific Ocean: Reconciling proxies and models. Earth Planet. Sci. Lett. 349–350, 53–66. https://doi.org/10.1016/j.epsl.2012.06.024.

Hollis, C.J., Dunkley Jones, T., Anagnostou, E., Bijl, P.K., Cramwinckel, M.J., Cui, Y., Dickens, G.R., Edgar, K.M., Eley, Y., Evans, D., Foster, G.L., Frieling, J., Inglis, G.N., Kennedy, E.M., Kozdon, R., Lauretano, V., Lear, C.H., Littler, K., Lourens, L., Meckler, A.N., Naafs, B.D.A., Pälike, H., Pancost, R.D., Pearson, P.N., Röhl, U., Royer, D.L., Salzmann, U., Schubert, B.A., Seebeck, H., Sluijs, A., Speijer, R.P., Stassen, P., Tierney, J., Tripati, A., Wade, B., Westerhold, T., Witkowski, C., Zachos, J.C., Zhang, Y.G., Huber, M., Lunt, D.J., 2019. The DeepMIP contribution to PMIP4: methodologies for selection, compilation and analysis of latest Paleocene and early Eocene climate proxy data, incorporating version 0.1 of the DeepMIP database. Geoscientific Model Develop. 12, 3149–3206. https://doi.org/10.5194/gmd-12-3149-2019.

Hönisch, B., Royer, D.L., Breecker, D.O., Polissar, P.J., Bowen, G.J., Henehan, M.J., Cui, Y., Steinthorsdottir, M., McElwain, J.C., Consortium, C. C. P. I. P. (CenCO2PIP), 2023. Toward a Cenozoic history of atmospheric CO2. Science 382 (6675), eadi5177. https://doi.org/10.1126/science.adi5177.

Hornibrook, N. De B., 1958, New Zealand foraminifera: key species in stratigraphy: New Zealand J. Geolog. Geophys., v. 1, p. 653-676.

Huber, M., Caballero, R., 2011. The early Eocene equable climate problem revisited. Clim. Past 7, 603–633. https://doi.org/10.5194/cp-7-603-2011.

Huber, B.T., Quillévéré, F., 2005. Revised Paleogene planktonic foraminiferal biozonation for the Austral Realm. J. Foraminifer. Res. 35, 299–314.

Huber, M., Brinkhuis, H., Stickley, C., Döös, K., Sluijs, A., Warnaar, J., Schellenberg, S.A., Williams, G., 2004. Eocene circulation of the Southern Ocean: was Antarctica kept warm by subtropical waters? Paleoceanography PA4026. https://doi.org/10.1029/PA001022.

Huck, C.E., van de Flierdt, T., Bohaty, S.M., Hammond, S.J., 2017. Antarctic climate, Southern Ocean circulation patterns, and deep water formation during the Eocene. Paleoceanography 32, 674–691. https://doi.org/10.1002/2017PA003135.

Inglis, G.N., Bragg, F., Burls, N.J., Cramwinckel, M.J., Evans, D., Foster, G.L., Huber, M., Lunt, D.J., Siler, N., Steinig, S., Tierney, J.E., Wilkinson, R., Anagnostou, E., De Boer, A.M., Dunkley Jones, T., Edgar, K.M., Hollis, C.J., Hutchinson, D.K., Pancost, R.D., 2020. Global mean surface temperature and climate sensitivity of the early Eocene Climatic Optimum (EECO), Paleocene–Eocene Thermal Maximum (PETM), and latest Paleocene. Clim. Past 16, 1953–1968. https://doi.org/10.5194/cp-16-1953-2020.

John, E.H., Pearson, P.N., Coxall, H.K., Birch, H., Wade, B.S., Foster, G.L., 2013. Warm ocean processes and carbon cycling in the Eocene. Philosophical Transactions of the Royal Society A: Mathematical, Physic. Engin. Sci. 371 (2001), 20130099. https://doi.org/10.1098/rsta.2013.0099.

John, E.H., Wilson, J.D., Pearson, P.N., Ridgwell, A., 2014. Temperature-dependent remineralization and carbon cycling in the warm Eocene oceans. Palaeogeogr. Palaeoclimatol. Palaeoecol. 413, 158–166. https://doi.org/10.1016/j.palaeo.2014.05.019.

Jonkers, L., Hillebrand, H., Kucera, M., 2019. Global change drives modern plankton communities away from the pre-industrial state. Nature 570, 372–375. https://doi.org/10.1038/s41586-019-1230-3.

Keller, G., MacLeod, N., Barrera, E., 1992. Eocene-oligocene faunal turnover in planktic foraminifera, and Antarctic glaciation. Eocene-Oligocene climatic and biotic evolution 218–246.

King, D.J., Wade, B.S., 2017. The extinction of Chiloguembelina cubensis in the Pacific Ocean: implications for defining the base of the Chattian (upper Oligocene). News. Stratigr. 311–339. https://doi.org/10.1127/nos/2016/0308.

Kirtland-Turner, S., Sexton, S., Charles, P., Norriss, R.D., 2014. Persistence of carbon release events through the peak of early Eocene global warmth. Nat. Geosci. 7, 748–751. https://doi.org/10.1038/ngeo2240.

Kucera, M., 2007. Chapter six planktonic foraminifera as tracers of past oceanic environments. In: Hillaire-Marcel, C., Vernal, A.D. (Eds.), Proxies in Late Cenozoic Paleoceanography, Developments in Marine Geology. Elsevier, pp. 213–262. https://doi.org/10.1016/S1572-5480(07)01011-1.

Lauretano, V., Hilgen, F.J., Zachos, J.C., Lourens, L.J., 2016. Astronomically tuned age model for the early Eocene carbon isotope events: A new high-resolution \ensuremath\delta13 Cbenthic record of ODP Site 1263 between \texttt\char126 49 and \texttt\char126 54 Ma. Newsletters on Stratigr. 49, 383–400. https://doi.org/10.1127/nos/2016/0077.

Leon-Rodriguez, L., Dickens, G.R., 2010. Constraints on ocean acidification associated with rapid and massive carbon injections: the early Paleogene record at ocean drilling program site 1215, equatorial Pacific Ocean. Palaeogeogr. Palaeoclimatol. Palaeoecol. 298, 409–420. https://doi.org/10.1016/j.palaeo.2010.10.029.

Littler, K., Röhl, U., Westerhold, T., Zachos, J.C., 2014. A high-resolution benthic stable-isotope record for the South Atlantic: Implications for orbital-scale changes in Late Paleocene–Early Eocene climate and carbon cycling. Earth Planet. Sci. Lett. 401, 18–30. https://doi.org/10.1016/j.epsl.2014.05.054.

Loeblich, A.R., Tappan, H., 1956. Chiloguembelina, a new Tertiary genus of the Heterohelicidae (Foraminifera). J. Wash. Acad. Sci. 46, 340.

Loeblich, A.R., Tappan, H., collaborators, 1957. Planktonic foraminifera of Paleocene and early Eocene Age from the Gulf and Atlantic coastal plains. In: Loeblich Jr., A.R. (Ed.), Studies in Foraminifera, 215. U.S. Natl. Museum Bull., pp. 173–198

Luciani, V., Giusberti, L., 2014. Reassessment of the Early-Middle Eocene planktic foraminiferal biomagnetochronology: New evidence from the Tethyan Possagno Section (Ne Italy) and Western North Atlantic Ocean ODP Site 1051. J. Foraminifer. Res. 44, 187–201. https://doi.org/10.2113/gsjfr.44.2.18.

Luciani, V., Dickens, G.R., Backman, J., Fornaciari, E., Giusberti, L., Agnini, C., D'Onofrio, R., 2016. Major perturbations in the global carbon cycle and photosymbiont-bearing planktic foraminifera \hack\newlineduring the early Eocene. Clim. Past 12, 981–1007. https://doi.org/10.5194/cp-12-981-201.

Luciani, V., D'Onofrio, R., Dickens, G.R., Wade, B.S., 2017a. Did Photosymbiont Bleaching Lead to the Demise of Planktic Foraminifer Morozovella at the early Eocene Climatic Optimum?: Early Eocene Photosymbiont Bleaching. Paleoceanography 32, 1115–1136. https://doi.org/10.1002/2017PA003138.

Luciani, V., D'Onofrio, R., Dickens, G.R., Wade, B.S., 2017b. Planktic foraminiferal response to early Eocene carbon cycle perturbations in the Southeast Atlantic Ocean (ODP Site 1263). Global Planet. Change 158, 119–133. https://doi.org/10.1016/j.gloplacha.2017.09.007.

Luciani, V., D'Onofrio, R., Filippi, G., Moretti, S., 2020a. Which was the habitat of early Eocene planktic foraminifer Chiloguembelina? Stable isotope paleobiology from the Atlantic Ocean and implication for paleoceanographic reconstructions. Global Planet. Change 191, 103216. https://doi.org/10.1016/j.gloplacha.2020.103216.

Luciani, V., Fornaciari, E., Papazzoni, C.A., Dallanave, E., Giusberti, L., Stefani, C., Amante, E., 2020b. Integrated stratigraphy at the Bartonian–Priabonian transition: Correlation between shallow benthic and calcareous plankton zones (Varignano

section, northern Italy). GSA Bull. 132, 495–520. https://doi.org/10.1130/B35169.1.
Martini, E., 1971. Standard Tertiary and Quaternary calcareous nannoplankton zonation. In: Farinacci, A. (Ed.), Proceedings 2nd International Conference Planktonic Microfossils Roma. Tecnoscienza, pp. 739–785.
McInerney, F.A., Wing, S.L., 2011. The paleocene-eocene thermal maximum: a perturbation of carbon cycle, climate, and biosphere with implications for the future. Annual Rev. Earth Pla. Sci. 39, 489–516. https://doi.org/10.1146/annurev-earth-040610-133431.
Miller, K.G., Browning, J.V., Schmelz, W.J., Kopp, R.E., Mountain, G.S., Wright, J.D., 2020. Cenozoic sea-level and cryospheric evolution from deep-sea geochemical and continental margin records. Sci. Adv. 6, eaaz1346. https://doi.org/10.1126/sciadv.aaz1346.
Morozova, V.G., 1939. Nadsemeistvo foraminifer Globigerinidea superfam. nova i nekotori yevo predstaviteli. Doklady Akademiya Nauk SSSR 114, 1109–1111.
Morozova, V.G., 1957. Nadsemeistvo foraminifer Globigernidea superfam. Nova I nekotori yevo predstaviteli: Doklady Akademiya Nauk SSSR 124, 1113–1116.
Müller, R.D., Zahirovic, S., Williams, S.E., Cannon, J., Seton, M., Bower, D.J., Tetley, M. G., Heine, C., Le Breton, E., Liu, S., Russell, S.H.J., Yang, T., Leonard, J., Gurnis, M., 2019. A global plate model including lithospheric deformation along major rifts and Orogens since the Triassic. Tectonics 38, 1884–1907. https://doi.org/10.1029/2018TC005462.
Nguyen, T.M.P., Speijer, R.P., 2014. A new procedure to assess dissolution based on experiments on Pliocene–Quaternary foraminifera (ODP Leg 160, Eratosthenes Seamount, Eastern Mediterranean). Mar. Micropaleontol. 106, 22–39. https://doi.org/10.1016/j.marmicro.2013.11.004.
Nguyen, T.M.P., Petrizzo, M.R., Speijer, R.P., 2009. Experimental dissolution of a fossil foraminiferal assemblage (Paleocene–Eocene Thermal Maximum, Dababiya, Egypt): Implications for paleoenvironmental reconstructions. Mar. Micropaleontol. 73, 241–258. https://doi.org/10.1016/j.marmicro.2009.10.005.
Nguyen, T.M.P., Petrizzo, M.R., Stassen, P., Speijer, R.P., 2011. Dissolution susceptibility of Paleocene–Eocene planktic foraminifera: Implications for palaeoceanographic reconstructions. Mar. Micropaleontol. 81, 1–21. https://doi.org/10.1016/j.marmicro.2011.07.001.
Norris, R.D., Turner, S.K., Hull, P.M., Ridgwell, A., 2013. Marine Ecosystem responses to Cenozoic Global Change. Science 341, 492–498. https://doi.org/10.1126/science.1240543.
Nuttall, W.L.F., 1930. Eocene foraminifera from Mexico. J. Paleo. 4, 271–293.
Olivarez Lyle, A., Lyle, M.W., 2006. Missing organic carbon in Eocene marine sediments: is metabolism the biological feedback that maintains end-member climates? Paleoceanography 21 (2). https://doi.org/10.1029/2005PA001230.
Olsson, R.K., Hemleben, Ch., Berggren, W.A., Liu, C., 1992. Wall texture classification of planktonic foraminifera genera in the lower Danian. J. Foraminifer. Res. 22, 195–213.
Olsson, R.K., Berggren, W.A., Hemleben, C., Huber, B.T., 1999. Atlas of Paleocene Planktonic Foraminifera. Smithsonian Contributions to Paleobiol. 1–252. https://doi.org/10.5479/si.00810266.85.1.
Pearson, P., Palmer, M., 2000. Atmospheric carbon dioxide concentrations over the past 60 million years. Nature 406, 695–699. https://doi.org/10.1038/35021000.
Pearson, P.N., Shackleton, N.J., Hall, M.A., 1993. Stable isotope paleoecology of middle Eocene planktonic foraminifera and multi-species isotope stratigraphy, DSDP Site 523, South Atlantic. J. Foram. Res. 23, 123–140. https://doi.org/10.2113/gsjfr.23.2.123.
Pearson, P.N., Ditchfield, P.W., Singano, J., Harcourt-Brown, K.G., Nicholas, C.J., Olsson, R.K., Shackleton, N.J., Hall, M.A., 2001. Warm tropical sea surface temperatures in the late cretaceous and Eocene epochs. Nature 413, 481–487. https://doi.org/10.1038/35097000.
Pearson, P.N., Olsson, R.K., Huber, B.T., Hemleben, C., Berggren, W.A., 2006. Atlas of Eocene Planktonic Foraminifera. Cushman Foundation Spec. Publ. Foram. Res. for Foram. Res, Greenville, NC, USA.
Petrizzo, M.R., Leoni, G., Speijer, R.P., De Bernardi, B., Felletti, F., 2008. Dissolution Susceptibility of some Paleogene Planktonic Foraminifera from ODP Site 1209 (Shatsky Rise, Pacific Ocean). J. Foraminifer. Res. 38, 357–371. https://doi.org/10.2113/gsjfr.38.4.357.
Poore, R.Z., Matthews, R.K., 1984. Oxygen isotope ranking of late Eocene and Oligocene planktonic foraminifers: implications for Oligocene Sea-surface temperatures and global ice-volume. Mar. Micropaleontol. 9, 111–134.
Premoli Silva, I., Boersma, A., 1988. Atlantic Eocene planktonic foraminiferal historical biogeography and paleohydrographic indices. Palaeogeogr. Palaeoclimatol. Palaeoecol. 67, 315–356. https://doi.org/10.1016/0031-0182(88)90159-9.
Pross, J., Contreras, L., Bijl, P.K., Greenwood, D.R., Bohaty, S.M., Schouten, S., Bendle, J. A., Röhl, U., Tauxe, L., Raine, J.I., Huck, C.E., van de Flierdt, T., Jamieson, S.S.R., Stickley, C.E., van de Schootbrugge, B., Escutia, C., Brinkhuis, H., 2012. Persistent near-tropical warmth on the Antarctic continent during the early Eocene epoch. Nature 488 (7409). https://doi.org/10.1038/nature11300. Article 7409.
Ridgwell, A., Zeebe, R.E., 2005. The role of the global carbonate cycle in the regulation and evolution of the Earth system. Earth Planet. Sci. Lett. 234, 299–315. https://doi.org/10.1016/j.epsl.2005.03.006.
Rohl, U., Westerhold, T., Monechi, S., Thomas, E., Zachos, J.C., 2005. The third and final early Eocene thermal maximum: Characteristics, timing, and mechanisms of the "X" event. Geol. Soc. of America 37, 264.
Schmidt, D., Thierstein, H., Bollmann, J., 2004. The evolutionary history of size variation of planktic foraminiferal assemblages in the Cenozoic. Palaeogeogr. Palaeoclimatol. Palaeoecol. 212, 159–180. https://doi.org/10.1016/S0031-0182(04)00312-8.
Sexton, P.F., Wilson, P.A., Pearson, P.N., 2006. Microstructural and geochemical perspectives on planktic foraminiferal preservation: "Glassy" versus "Frosty". Geochem. Geoph. Geosyst. 7. https://doi.org/10.1029/2006GC001291.
Shipboard Scientific Party, 1990. Site 762. Proc. Oc. Drill. Progr., Initial Rep, 122, pp. 213–289.
Siesser, W., Bralower, T.J., 1992. Cenozoic calcareous nannofossil biostratigraphy on the Exmouth Plateau, Eastern Indian Ocean. Proc. Oc. Drill. Prog. Scient. Res. 122, 601–631.
Shamrock, J.L., Watkins, D.K., Johnston, K.W., 2012. Eocene biogeochronology and magnetostratigraphic revision of ODP Hole 762C. Exmouth Plateau (northwest Australian Shelf) 9.
Slotnick, B., Dickens, G., Nicolo, M.J., Hollis, C.J., Crampton, J.S., Zachos, J.C., 2012. Large-amplitude variations in carbon cycling and terrestrial weathering during the latest Paleocene and Thomas, E., 2007. Cenozoic mass extinctions in the deep sea: what perturbs the largest habitat on earliest Eocene: The record at Mead Stream. New Zealand J. Geol. Geoph. 120 (5), 487–505. https://doi.org/10.1086/666743.
Slotnick, B., Dickens, G., Hollis, C., Crampton, J., Percy Strong, C., Phillips, A., 2015. The onset of the Early Eocene Climatic Optimum at Branch Stream, Clarence River valley, New Zealand. New Zealand J. Geol. Geoph. 58, 262–280. https://doi.org/10.1080/00288306.2015.1063514.
Speijer, R., Scheibner, C., Stassen, P., Morsi, A.-M., 2012. Response of marine ecosystems to deep-time global warming: A synthesis of biotic patterns across the Paleocene-Eocene thermal maximum (PETM). Austrian J. Earth Sci. 105, 6–16.
Subbotina, N.N., 1953. Fossil Foraminifera of the USSR: Globigerinidae, Hantkeninidae and Globorotalidae., Translation to English by E. Lees. Collet's Ltd., London and Wellingborough, v, 76 (in Russian), 296 p. (translat. 321 p.).
Sutherland, R., Dickens, G.R., Blum, P., the Expedition 371 Scientists., 2018. Expedition 371 preliminary report: Tasman frontier subduction initiation and paleogene climate. International Ocean Discovery Program. https://doi.org/10.14379/iodp.pr.371.2018.
Sutherland, R., Dickens, G., Blum, P., 2019a. Tasman frontier subduction initiation and paleogene climate. Proc. Oc. Drill. Sci. Res. https://doi.org/10.14379/iodp.proc.371.2019.
Sutherland, R., Dickens, G., Blum, P., Agnini, C., Alegret, L., Bhattacharya, J., Aurelien, B., Chang, L., Collot, J., Cramwinckel, M., Dallanave, E., Drake, M., Etienne, S., Giorgioni, M., Gurnis, M., Harper, D., Huang, H.-H., Keller, A., Lam, A., Zhou, X., 2019b. Tasman frontier subduction initiation and paleogene climate. I. Oc. Drill. Prog.: Prel. Rep. 1–44.
Swain, A., Woodhouse, A., Fagan, W.F., Fraass, A.J., Lowery, C.M., 2024. Biogeographic response of marine plankton to Cenozoic environmental changes. Nature 629, 616–623. https://doi.org/10.1038/s41586-024-07337-.
Thomas, E., 1998. Biogeography of the Late Paleocene benthic foraminiferal extinction. Env. Sci. 21, 214–243.
Thomas, E., 2007. Cenozoic mass extinctions in the deep sea: What perturbs the largest habitat on Earth? In: Monechi, S., Coccioni, R., Rampino, M. (Eds.), Large Ecosystem Perturbations: Causes and Consequences. Geological Society of America. https://doi.org/10.1130/2007.2424(01), p. 0.
Thomas, E., Shackleton, N., Hall, M., 1992. Data Report: Carbon Isotope Stratigraphy of Paleogene Bulk Sediments, Hole 762C (Exmouth Plateau, Eastern Indian Ocean). Proc. Oc. Drill. Sci. Res. 122. https://doi.org/10.2973/odp.proc.sr.122.195.1992.
Thomas, E., Boscolo-Galazzo, F., Balestra, B., Monechi, S., Donner, B., Rohl, U., 2018. Early Eocene thermal maximum 3: Biotic response at Walvis Ridge (SE Atlantic Ocean). Paleoceanogr. Paleoclimatol. 33, 862–883. https://doi.org/10.1029/2018PA003375.
Van Hinsbergen, D.J.J., de Groot, L.V., van Schaik, S.J., Spakman, W., Bijl, P.K., Sluijs, A., Langereis, C.G., Brinkhuis, H., 2015. A Paleolatitude Calculator for Paleoclimate Studies. PloS One 10 (6), 1–21. https://doi.org/10.1371/journal.pone.0126946.
Wade, B.S., Pearson, P.N., Berggren, W.A., Pälike, H., 2011. Review and revision of Cenozoic tropical planktonic foraminiferal biostratigraphy and calibration to the geomagnetic polarity and astronomical time scale. Earth Sci. Rev. 104, 111–142. https://doi.org/10.1016/j.earscirev.2010.09.003.
Westerhold, T., Röhl, U., Frederichs, T., Agnini, C., Raffi, I., Zachos, J.C., Wilkens, R.H., 2017. Astronomical calibration of the Ypresian timescale: implications for seafloor spreading rates and the chaotic behavior of the solar system? Clim. Past 13, 1129–1152. https://doi.org/10.5194/cp-13-1129-2017.
Westerhold, T., Röhl, U., Donner, B., Zachos, J.C., 2018. Global extent of early eocene hyperthermal events: A new pacific benthic foraminiferal isotope record from Shatsky rise (ODP Site 1209). Paleoceanogr. Paleoclimatol. 33, 626–642. https://doi.org/10.1029/2017PA003306.
Wilson, J.D., Monteiro, F.M., Schmidt, D.N., Ward, B.A., Ridgwell, A., 2018. Linking marine plankton ecosystems and climate: A new modeling approach to the warm early Eocene climate. Paleoceanogr. Paleoclimatology 33 (12), 1439–1452. https://doi.org/10.1029/2018PA003374.
Wonders, A.A.H., 1992. Cretaceous Planktonic Foraminiferal Biostratigraphy, Leg 122, Exmouth Plateau, Australia. Proc. Oc. Drill. Sci. Res. 587–599.
Woodhouse, A., Jackson, S.L., Jamieson, R.A., Newton, R.J., Sexton, P.F., Aze, T., 2021. Adaptive ecological niche migration does not negate extinction susceptibility. Scient. Rep. 11.
Xu, K., De Vleeschouwer, D., Vahlenkamp, M., Yang, R., Chen, H., 2021. Reconstructing Eocene Eastern Indian Ocean dynamics using ocean-drilling stratigraphic records.

Paleoceanogr. Paleoclimatology 36. https://doi.org/10.1029/2020PA004116 e2020PA004116.

Zachos, J.C., Röhl, U., Schellenberg, S.A., Sluijs, A., Hodell, D.A., Kelly, D.C., Thomas, E., Nicolo, M., Raffi, I., Lourens, L.J., McCarren, H., Kroon, D., 2005. Rapid acidification of the ocean during the paleocene-eocene thermal maximum. Science 308, 1611–1615. https://doi.org/10.1126/science.1109004.

Zachos, J.C., McCarren, H., Murphy, B., Röhl, U., Westerhold, T., 2010. Tempo and scale of late Paleocene and early Eocene carbon isotope cycles: Implications for the origin of hyperthermals. Earth Planet. Sci. Lett. 299 (1), 242–249. https://doi.org/10.1016/j.epsl.2010.09.004.